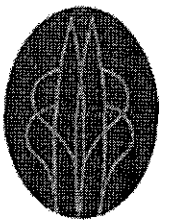

UNIVERSITI
TEKNOLOGI
PETRONAS

Compression Capacity Prediction of Cold-Formed Steel Sections

by

Natasya Ng Jia Weyn

Dissertation submitted in partial fulfilment of
the requirements for the
Bachelor of Engineering (Hons)
(Civil Engineering)

JULY 2008

Universiti Teknologi PETRONAS
Bandar Seri Iskandar
31750 Tronoh
Perak Darul Ridzuan

CERTIFICATION OF APPROVAL

Compression Capacity Prediction of Cold-Formed Steel Sections

by

Natasya Ng Jia Weyn

A project dissertation submitted to the
Civil Engineering Programme
Universiti Teknologi PETRONAS
in partial fulfilment of the requirement for the
BACHELOR OF ENGINEERING (Hons)
(CIVIL ENGINEERING)

Approved by,

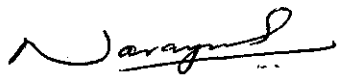

(AP Dr. Narayanan Sambu Potty)

UNIVERSITI TEKNOLOGI PETRONAS

TRONOH, PERAK

July 2008

CERTIFICATION OF ORIGINALITY

This is to certify that I am responsible for the work submitted in this project, that the original work is my own except as specified in the references and acknowledgements, and that the original work contained herein have not been undertaken or done by unspecified sources or persons.

NATASYA NG JIA WEYN

ABSTRACT

Cold-formed steel sections have important advantages such as flexible cross sectional profiles and high strength-to-weight ratio but constantly experience buckling problems. They are currently designed based on Effective Width philosophy in the BS, Euro, American and Australian codes. The Direct Strength Method is a new design philosophy utilizing the buckling loads obtained from a buckling analysis. This project aims to investigate the feasibility of using the Direct Strength method especially when employing the sections available in Malaysia industry. The local steel designers are not well exposed to this method and no study has been reported on its use in local industry. Activities of the project include data gathering, column buckling analysis using Cornell University Finite Strip Method (CUFSM) and comparison of ultimate strength based on test values and applications of Direct Strength method and Effective Width method. Compression testing on Bluescope Lysaght sections C15015, C15019, Z15015 and Z15019 of 500 mm and 1000 mm length were carried out and were analyzed. Comparison with test results shows good agreement with the theoretical values predicted using Direct Strength method. This method can be a good compression capacity predictor because it explicitly incorporates all buckling modes, does not require calculations of effective properties and gives reliable predictions.

ACKNOWLEDGEMENT

The author is taking this opportunity to express her gratitude to all the parties who gave her the possibility to complete this project. Sincere thanks go to the respectable Supervisor, AP. Dr. Narayanan Sambu Potty, who has supported the author by his guidance and encouragement which made the author's research a wonderful learning experience. Without him, the author could not have fulfilled her goal to such a great extent.

Special notes of thanks also go to the FYP Coordinator, Mr. Kalaikumar a/l Vallyutham for his monitoring of the whole project progress. The author was also honored to work with several individuals who have contributed their practical experience and skills in the testing work, these being technicians Mr. Johan Ariff, Mr. Hafiz, and Mr. Meow Asniwan.

The author would also like to thank Mr. Chong Kok Cheong and Mr. Jeeva and from BlueScope Steel Malaysia Sdn. Bhd. for their kind assistance in supplying the steel samples needed for the testing. Without the sponsorship of the company, the author could not have advanced to another stage.

The author is thoroughly indebted to the aforesaid individuals as well as to all other people who have helped in the completion of this project.

TABLE OF CONTENTS

LIST OF TABLES

LIST OF FIGURES

ABBREVIATIONS AND NOMENCLATURES

A	-	Gross area of a cross section
A_e	-	Effective net area of a section
A_{eff}	-	Effective area
A_n	-	Net area of a section
B	-	Overall width of an element
b	-	Flat width of an element
b_{eff}	-	Effective width of a compression element
b_{eu}	-	Effective width of an unstiffened compression element
C_b	-	Coefficient defining the variation of moments on a beam
C_W	-	Warping constant of a section
D	-	Overall web depth
E	-	Modulus of elasticity of steel
e	-	Distance between a load and a reaction
e_s	-	Distance between the geometric neutral axis and the effective neutral axis of a section
F_c	-	Applied axial compressive load
f_c	-	Compressive stress on the effective element
G	-	Shear modulus of steel
I	-	Second moment of area of a cross section about its critical axis
I_x	-	Second moment of area of a cross section about the x-axis
I_y	-	Second moment of area of a cross section about the x-axis
J	-	Torsion constant of a section
K	-	Buckling coefficient of an element
L	-	Length of a member between support points
L_E	-	Effective length of a member
M	-	Applied moment on a beam
M_c	-	Moment capacity of a cross section
M_{crd}	-	Critical elastic distortional buckling moment
M_{cre}	-	Critical elastic lateral-torsional buckling moment
M_{crl}	-	Critical elastic local buckling moment

M_E	-	Elastic lateral buckling moment of a beam
M_{ne}	-	Nominal flexural strength for lateral-torsional buckling
M_x	-	Moment about x-axis
M_y	-	Moment about y-axis
P_c	-	Buckling resistance under axial load
P_{cs}	-	Short strut capacity
P_{crd}	-	Critical elastic distortional column buckling load
P_{cre}	-	Critical elastic column buckling load
P_{crl}	-	Critical elastic local column buckling load
P_E	-	Elastic flexural buckling load (Euler load) for a column
P_{ne}	-	Flexural, torsional, or torsional-flexural buckling strength
p_c	-	Compressive strength
p_{cr}	-	Local buckling stress of an element
p_y	-	Design strength of steel
r	-	Radius of gyration
t	-	Net material thickness
x	-	Torsional constant
Y_s	-	Nominal yield strength of steel
v	-	Poisson ratio
λ_l	-	local slenderness
λ_d	-	distortional slenderness

CHAPTER 1
INTRODUCTION

1.1 Background of Study

Structural design aims to provide, with due regard to economy, a structure capable of fulfilling its proposed function and sustaining the design loads for its intended life. In economy wise, the weight of the material must be kept minimum to achieve low erection cost and cold-formed steel structural members could fulfil this condition. Cold-formed steel structural members provide various kinds of cross sections with the right purpose, and can be produced economically by using selective forming operations. They provide a much large variety of choices for steel designers.

Cold-formed steel structures are made from structural elements by bending flat sheets at ambient temperatures into shapes which will support loads. In the past cold-formed thin-walled steel sections were used generally for products where weight saving was of chief importance, e.g. in the aircraft, railway and motor industries. Simple types of cold-formed profiles and profiled sheeting have also been used as non-structural elements in building for about one hundred years.

In recent years, cold-formed steel has become a popular structural alternative to timber and concrete and is used extensively in low-rise buildings. It is utilized in a variety of applications, supporting floors, roofs and walls in industrial, commercial and residential buildings. Several factors such as systematic research work, improved manufacturing technology, protection against corrosion, increased material strength and the availability of codes of practice for design have contributed to the fast growing of cold-formed steel construction.

In the past decades, cold-formed steel has been brought into Malaysian construction. It is a steel work technology that can offer advantages such as high strength-to-weight ratio, optimisation of various cross sectional shapes and fast erection. Imported or locally made steel products are adopted in construction industry nowadays and they have been adapted for local conditions. They are locally produced to meet the high standards demanded, and also cope well with harsh and humid weather conditions.

1.2 Problem Statement

Cold-formed steel members always encounter many types of instabilities because they are thin and light. Thus, designers must consider the various classes of instability such as local, distortional and global buckling when designing a cold-formed steel structure.

Traditionally, the cold-formed steel design is based on AISI Specification (AISI, 1996) and BS5950 Part 5 (BSI, 1987). However, Newman (1997) said, "anyone who has ever attempted to design a light-gauge member following the Specification provisions probably realized how tedious and complex the process was. When such [cold-formed] framing is needed one of two things tends to happen to the engineers: they either uncritically rely on the suppliers' literature, or simply avoid any cold-formed design at all." Besides, the Effective Width method which is intimately tied to classical plate stability has several flaws that hinder its use in cold-formed steel design.

Recent developments in cold-formed steel industry have heightened the need for a simpler and more practical method to design cold-formed steel structures. Engineered solution that offers greater choices of structural layout, functions and aesthetic quality are preferred by more clients.

In recent years Schafer (2006) has developed a new method, namely Direct Strength Method to integrate computational stability analysis into the design process in order to ease the design process and to encourage the manufacturing of innovative cross sections.

In Malaysia, BS5950 Part 5 (BSI, 1998) is currently used by the engineers for design of cold-formed steel structures. Limited studies have been carried out in Malaysia on cold-formed structures (Tahir, Tan, & Shek, 2006; Tahir, Thong, & Tan, 2005). In addition, far too little attention has been paid to the Direct Strength method. No research has been found that surveyed the feasibility and reliability of this method using locally made steel products.

It is worthwhile to look into the various cold-formed steel cross sections produced locally and analyze their buckling mode and load. Elastic buckling results can be viewed as another gross property of the cross section. This stability analysis of cold-formed steel sections in Malaysia could aid the engineers in designing cold-formed structures in the future.

1.3 Aim and Objectives

The aim of the study is to investigate the feasibility of the Direct Strength Method especially when using locally made cold-formed steel products. The following objectives would be considered to reach the aim:

- To compare the experimental results of the cold-formed steel section compression test reported in the literature with the member strength calculated by using Direct Strength method and Effective Width method
- To compare laboratory results of locally produced cold-formed steel section compression test with the member strength calculated by using the Direct Strength method and Effective Width method
- To bring out guidelines facilitating the use the Direct Strength method and its acceptance among local users

1.4 Scope of Study

The study focused on the cold-formed steel cross sections that are imported and locally produced in Malaysia. There were three major stages during this study:

i. Data gathering

   All relevant data of cold-formed steel and the steel products being manufactured or used in Malaysia were acquired.

ii. Buckling behaviour analysis

   The buckling mode and critical load of all the cold-formed steel cross sections identified above were analyzed by using software called CUFSM.

iii. Laboratory experiments

   Limited compression tests on the cold-formed steel cross sections were carried out to compare the experimental results with the calculated member capacity.

1.5 Structure of Report

The report is divided into five chapters and each can be generally summarized as below:

i. Chapter 1 includes a background of cold-formed steel. It also consists of the problem statement, aims and objectives and lastly the scope of study

ii. Chapter 2 describes cold-formed steel in general and covers the Effective Width method and the Direct Strength method

iii. Chapter 3 explains the methodology for the study and includes a hazard analysis

iv. Chapter 4 details the results and discussions of a few selected cold-formed steel sections that were reported in literature and included in the compression test

v. Chapter 5 concludes the study according to the objectives that have been clarified in section 1.3. It also states the general conclusion and gives suggestions about the study.

CHAPTER 2
LITERATURE REVIEW

2.1 Brief Overview of Cold-Formed Steel

Cold-formed steel structural member is shape manufactured by press-braking blanks sheared from sheets, cut lengths of coils or plates, or by roll forming cold- or hot-rolled coils or sheet. Both forming operations are being performed at ambient room temperature, that is, without manifest addition of heat such as would be required for hot forming. A variety of steel thickness is available to meet a wide range of structural and non-structural applications. Figure 2.1 shows the typical cold-formed steel shapes.

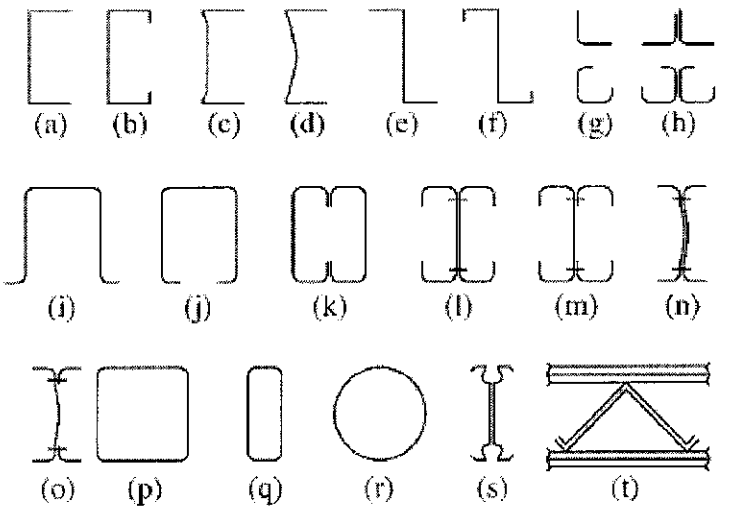

Figure 2.1 Cold-formed sections used in structural framing (Adapted from (Yu, 2000))

Three methods are generally used in the manufacture of cold-formed sections:

- cold roll forming
- press brake operation
- bending brake operation

The machine used in cold roll forming consists of pairs of rolls which progressively form strips into the final required shape. Each pair of rolls produces a fixed amount of deformation in a sequence. A simple section may be produced by as few as six pairs of rolls. However, a complex section may require as many as 15 sets of rolls. Roll setup time may be several days. This manufacture process is more popular for producing large quantities of a given shape.

Brake forming requires producing one complete fold at a time along the full length of the section, using a machine called a press brake. It is essential to move the steel plate in the press and to repeat the breaking operations a few times for sections with several folds. The finished section is subsequently removed from the press and a new piece of plate is placed for manufacture of the next section (Hancock, Murray, & Ellifritt, 2001).

In building construction, cold-formed steel products can be classified into three categories: members, panels, and prefabricated assemblies. Typical cold-formed steel members such as studs, track, purlins, girts and angles are mainly used for carrying loads while panels and decks constitute useful surfaces such as floors, roofs and walls, in addition to resisting the in-plane and out-of-plane surface loads. Prefabricated cold-formed steel assemblies include roof trusses, panelized walls or floors, and other prefabricated structural assemblies. Approximately 40% of the total steel used in building construction in U.S. is cold-formed steel.

In general, cold-formed steel structural members provide the following advantages in building construction (Yu, 2000):

- As compared with thicker hot-rolled shapes, cold-formed light members can be manufactured for relatively light loads and/ or short spans.
- Unusual sectional configurations can be produced economically by cold-forming operations, and consequently favorable strength-to-weight ratios can be obtained.
- Nestable sections can be produced, allowing for compact packaging and shipping.

- Load-carrying panels and decks can provide useful surfaces for floor, roof, and wall construction, and in other cases they can also provide enclosed cells for electrical and other conduits. They not only withstand loads normal to their surfaces, but they can also act as shear diaphragms to resist force in their own planes if they are adequately interconnected to each other and to supporting members.

The application of cold-formed steel members offers many advantages as compared with construction using hot-rolled steel. Table 2.1 below shows the comparison between these two steel elements.

Table 2.1 Comparison between hot-rolled steel and cold-formed steel

Aspect	Hot-rolled steel	Cold-formed steel
Design code and standard	AISC Steel Construction Manual (AISC, 1993)	AISI Cold-Formed Steel Design Manual (AISI, 1996)
Behavior and failure mode	It rarely exhibits local buckling.	It can experience local instabilities that do not normally lead to failure, but are helped by post-buckling strength.
Manufacture process	It is passed through a set of work rolls at elevated temperature in molten form.	It is formed at room temperature from cold strips or sheets using techniques such as folding, press braking, and cold rolling.
Effect of manufacture process	Minimal effect on the properties of steel.	Properties e.g. yield stress, ultimate strength and ductility are altered by the bending radius, thickness of the sheet, type of steel and the forming process.
Section shapes	More standardized.	Less standardization of shapes; readily varied for its application

Aspect	Hot-rolled steel	Cold-formed steel
Fastening method	Usually are connected with bolts or welds.	May be connected with bolts, screws, puddle welds, pop rivets, mechanical seaming, and "clinching".
Production cost	Higher cost in equipment, e.g. handling of heavy billets, the need to reheat the steel sections, the heavy rolling stands, and the loading, stacking and storage of the finished product.	Less cost in equipment. High initial tooling costs for roll forming.

Other advantages of cold-formed steel sections over hot-rolled steel, timber sections and concrete are listed in the paper written by Tahir, Thong, & Tan (2005).

2.2 Elastic Buckling of Cold-Formed Steel Section

Buckling is a limit state of sudden change in the geometry of a structure or any of its elements under a critical loading condition. Buckling mode is the shape that a member buckles into. More accurately, a buckling mode symbolizes a secondary deformed shape that has the same potential energy as the primary deformation.

Finite strip analysis (Cheung & Tham, 1998) provides an alternative to conventional finite element analysis that is nicely suited for exploration of cross section stability. Finite strip analysis of a cold-formed steel lipped channel in pure compression (Figure 2.2) shows that for practical member lengths all modes occur at stresses low enough that they must be considered in understanding and predicting behavior. Therefore, in addition to usual considerations for columns: material non-linearity (e.g., yielding), imperfections, residual stresses, etc., the individual role and potential for interaction of buckling modes must also be considered (Schafer, 2001).

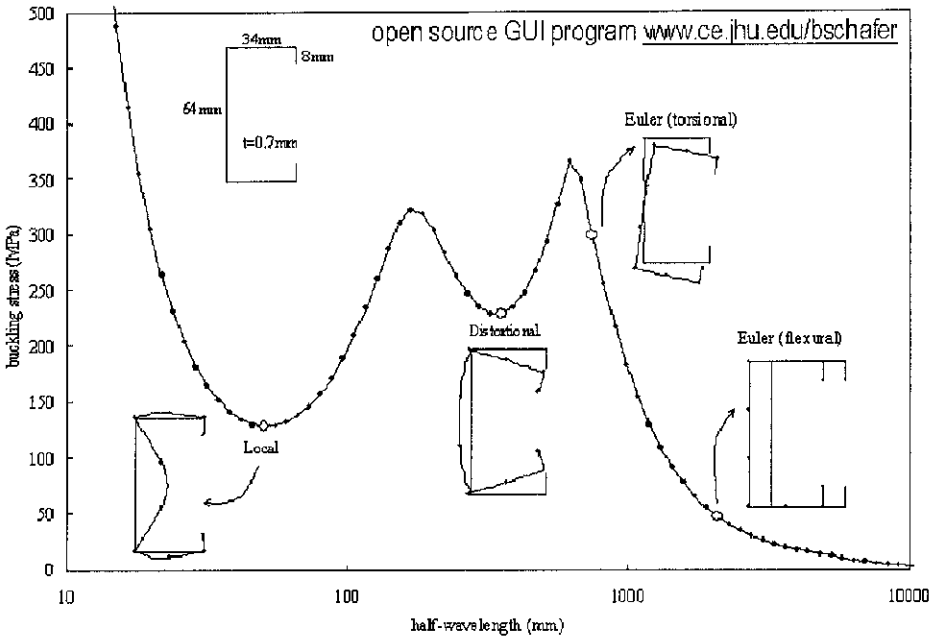

Figure 2.2 Finite strip analysis of a lipped channel in compression (Adapted from (Schafer, 2001))

As the finite strip analysis of Figure 2.2 demonstrates, stability of cold-formed steel members can typically be categorized into one of three classes: global or flexural Euler (G), distortional (D), or local (L). As defined in the Australian/New Zealand Standard (AS/NZS, 1996), local buckling is a mode involving plate flexure alone without transverse deformation of the line or lines of intersection of adjoining plates. As width-to-thickness ratios (*w/t*) increase local buckling stress decreases. Figure 2.3 shows how these thin elements may buckle locally when they are subjected to compression in flexural bending and axial compression.

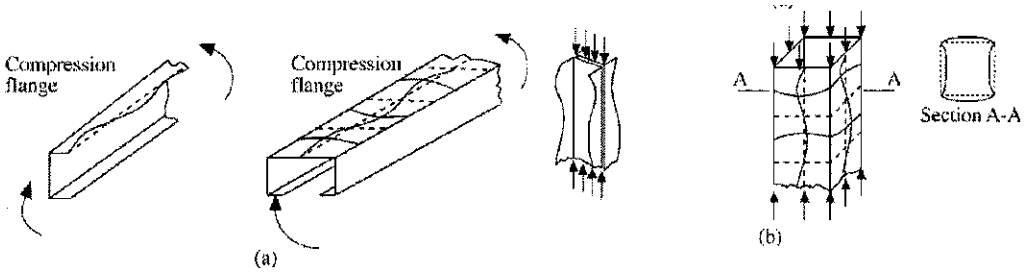

Figure 2.3 Local buckling of compression elements (a) beams (b) columns (Adapted from (Yu, 2000))

Distortional buckling is a mode of buckling involving change in cross sectional shape excluding local buckling. In members with edge stiffened elements, this mode involves a rotation of the flange at the flange/web junction whereas in members with intermediately stiffened elements, it is distinguished by displacement of the intermediate stiffener normal to the plane of the element (Schafer, 2000). Figure 2.4 shows a few examples of distortional buckling experienced by lipped C-section, hat section and Z-section.

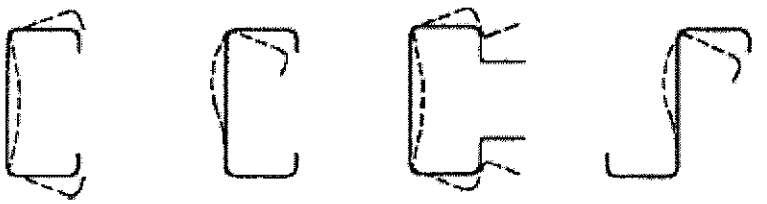

Figure 2.4 Examples of distortional buckling
(Adapted from Chodraui et al. (2006))

Flexural-torsional (sometimes called torsional-flexural) is a mode in which compression members can bend and twist simultaneously without change of cross sectional shape. Cold-formed open section steel members are more likely to undergo torsional deformation due to their low torsional rigidity resulting from their thin walls. Further, the sections are often loaded eccentrically from their shear centres and so are subjected to substantial torques as shown in Figure 2.5 (Hancock, 2003).

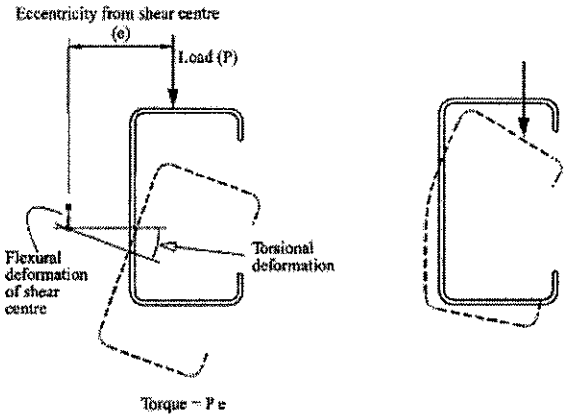

Figure 2.5 Torsional and distortional deformations of channel sections
(Adapted from (Hancock, 2003))

Although the terms global, distortional and local buckling mentioned beforehand are broadly used in the literature, there is no widely adopted method which provides buckling stresses for all the three characteristic modes. Moreover, there are no generally applicable and comprehensible classifications for the various modes themselves. The preceding definitions work well for a number of practical problems however they are not exact enough in many other cases (Schafer & Ádány, 2005).

A handy means for classification of the buckling class is the minima of the conventional finite strip analysis results. Minima in the buckling curves that fall at half-wavelengths less than the largest characteristic dimension of the member are considered as local buckling modes. Buckling modes occurring at longer lengths are either distortional or global in nature. However, this definition is by no means general and depends on the details of the cross section and loading. Sometimes minima may not exist, or extra minima may exist (Schafer & Ádány, 2006). Besides, the flexural and distortional buckling may interact at relatively long half-wavelengths thus long column modes at intermediate to long lengths are hard to be identified.

2.3 Finite Strip Analysis and CUFSM

In the finite strip method (FSM) cold-formed steel member, such as the lipped channel of Figure 2.6, is discretized into longitudinal strips. The advantage of FSM over other methods, such as the finite element method which applies discretization in both the longitudinal and transverse direction, is dependent on a judicious choice of the shape function for the longitudinal displacement field.

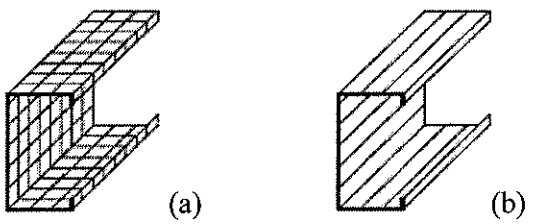

Figure 2.6 Finite strip discretization (a) finite element (b) finite strip (Adapted from (Schafer & Ádány, 2006))

FSM can now be completed straightforwardly due to immense advance of computer usage. A designer can perform finite strip analysis of any cross section with ease. Incorporation of this method in the open source code Cornell University Finite Strip Method (hereafter mentioned as CUFSM) (Schafer, 2004) allows the user to analyze the buckling stress and buckling mode of arbitrarily shaped, simply supported cold-formed steel members. In many cases, the first minimum point of the curve identifies the local buckling, while the second minimum point is often associated with the distortional buckling mode. However examples exist where FSM does not automatically identify minima.

While traditional hand methods used for plate structures regularly ignore compatibility at plate junctures and generally provide no means to calculate a variety of important buckling modes, CUFSM allows all elastic buckling modes of a structure to be quantified and examined (Schafer & Ádány, 2006).

However, FSM also have several restrictions, such as the cross section of the member cannot vary along the length, loads applied on the member cannot vary along the length (i.e., no moment gradient) and the global boundary conditions at the member ends must be pinned (i.e., simply-supported).

2.4 Effective Width Method

When analyzing the load-bearing behavior and estimating the failure load of a cold-formed member the effective width of the elements will be considered. As cold-formed members have very high width-to-thickness ratios, they tend to buckle elastically under low compressive stress. However, for plate that is supported along its edges or stiffened by some element, the stiffened edges of the plate remain stable and a certain width of the plate close to the corners is still effective in resisting further compressive load. The stress distribution of a simply supported plate strip under normal forces is illustrated in Figure 2.7. It is apparent that in the post-buckling range the stresses are concentrated along the plate supports.

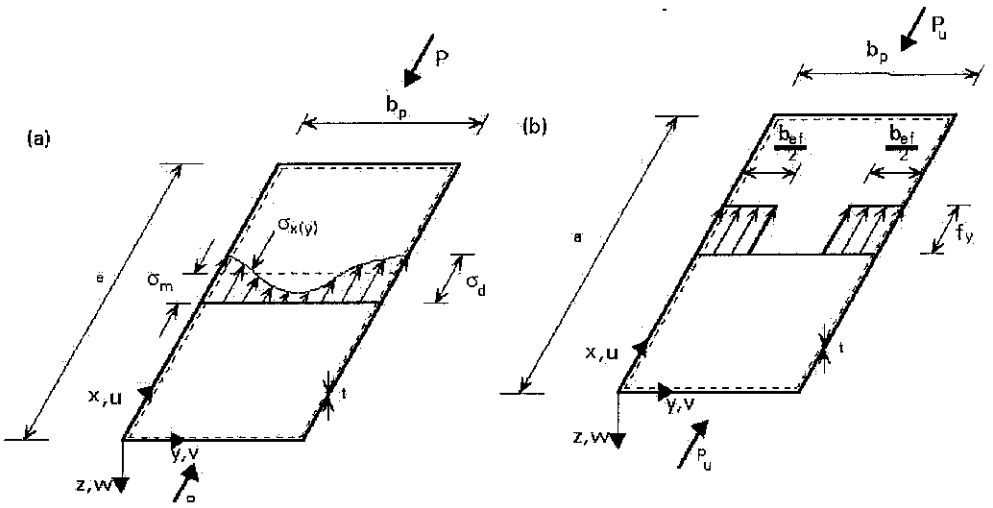

Figure 2.7 Stress distribution (a) over a doubly supported plate, and (b) the appropriate effective width approach (Source: http://www.kuleuven.be/bwk/materials/Teaching/master/wg09/l0200.htm)

The force *P* acting a simply supported plate strip is

$$P = \int_a^b \sigma_{x(y)} t . dy = \sigma_m b_p \qquad (1)$$

Von Karman (Von Karman, Sechler, & Donnell, 1932) proposed that the stress distribution at the central section of a stiffened plate be substituted by two widths *b/2* on each side of the plate, each subjected to a uniform stress f_y such that:

$$P_u = f_y b_{ef} t \qquad (2)$$

The segment of the original width of the plate that is still effective is called effective width whereas the strength left in the plate is called post-buckling strength. Subsequently, the ultimate load can be determined from a uniform stress distribution within an effective width b_{ef}, which depends on the critical buckling stress σ_{cr} and the yield stress f_y of the plate material.

$$b_{ef} = f(\sigma_{cr}, f_y) \qquad (3)$$

$$\frac{b_{ef}}{b_p} = \sqrt{\frac{\sigma_{cr}}{f_y}} \qquad (4)$$

This philosophy is named as Effective Width method. Then, in order to take into account of the geometric imperfections and residual stresses from the cold-forming operation, Winter has proposed the following effective width formulae for stiffened and unstiffened compression element:

$$P = \frac{b_{ef}}{b_p} = \sqrt{\frac{\sigma_{cr}}{f_y}}\left(1 - 0.22\sqrt{\frac{\sigma_{cr}}{f_y}}\right) \qquad (5)$$

These effective width formulas were published in the first Cold-Formed Specification in 1946 and remained unaltered until 1986. In the 1986 edition of the specification, all compression elements are treated with an effective width approach not considering if the member is stiffened or unstiffened. Plate buckling constant, k is used in effective width equation to separates one element from another. For example, a plate with simply supported edges on all four sides and subjected to uniform compression will buckle at a half-wavelength w with $k = 4.0$.

Reduction from the gross cross section to the effective cross section is fundamental to the application of the Effective Width method. The effective cross section (i) provides an apparent representation for the locations in the cross section where material is ineffective in carrying load, (ii) plainly explains the neutral axis shift in the section due to local-buckling and (iii) provides an obvious means to incorporate local–global interaction where reduced cross section properties influence global buckling (Schafer, 2008).

Nevertheless, the Effective Width method has been proven to have several limitations by the researchers (Schafer, 2001). First of all, the two-dimensional nonlinear stress distribution that is shown to explain the effective width of a plate is an approximation, representing the average of the longitudinal membrane stress and ignoring variation in stress through the thickness as well as variation in stress along the length of the plate. Thus, the true "effective width" is far more complicated than typically assumed and existing effective width equations only correlate to average membrane stress conditions in a plate (Schafer, 2008). Secondly, as sections become more complex with additional edge and intermediate stiffeners, the computation of the effective widths become more complex. Besides, cumbersome iteration needs to be carried out to determine the member strength.

In addition, Effective Width method is typically used to design members with slender elements. As such, members are idealized as a composition of plates with known boundary conditions, and slenderness limits or effective widths are appropriately derived for each element. Element interaction, the necessity for equilibrium and compatibility between any two elements of a cross section to be maintained, is often ignored or only included in an ad hoc manner in the AISC Specification. Research has shown that element interaction could be noteworthy in some cross sections, and that the issue is of growing importance for higher strength steels. As a result, consideration of elements in isolation is less accurate.

Lastly, Effective Width method does not explicitly consider distortional buckling. Experimental and numerical studies have indicated that post-buckling strength in the distortional mode is less than in the local mode, distortional failures may control the failure mechanism even when the elastic distortional buckling stress f_{crd} is higher than the elastic local buckling stress f_{crl} and distortional failures have higher imperfection sensitivity (Schafer & Peköz, 1998). Hence when distortional buckling and local buckling are treated separately in this method, inaccuracy in member strength predict will exist.

2.5 Direct Strength Method

A new design method utilizing the buckling loads obtained from a buckling analysis and direct strength equations has been developed (Schafer & Peköz, 1998(b)). This method accounted for distortional buckling of thin-walled sections (Hancock, Kwon, & Bernard, 1994). Incorporation of this method in the Australian/New Zealand Standard for Cold-Formed Steel Structures (AS/NZS, 1996) has led to successful prediction of the distortional buckling strength of flexural and compression members.

Direct Strength method (DSM) was first formalized for cold-formed steel beams undergoing local or distortional buckling (Schafer & Peköz, 1998(b)) and then for pin-ended columns in local, distortional or flexural-torsional buckling (Schafer, 2002). DSM reliability which is based on 267 column tests and 569 beam tests equals existing design methods because comparisons with existing design methods have been encouraging. To add to its achievement, this method has recently been accepted for cold-formed steel beams and columns as a new alternative method in the 2004 supplement to the AISI North American Specification (AISI, 2004).

From the buckling analysis, the elastic buckling loads and/or moments involved in the buckling of members are determined. For columns this includes the local, distortional and overall buckling loads whereas for beams this includes the local, distortional and overall buckling moments. Based on the elastic buckling behavior, DSM uses a series of strength curves to predict the member strength.

In order to use DSM, the users must be aware of the cross sections employed to verify the approach. Cold-formed steel sections must fulfill certain geometric requirement. A wide-ranging testing on cold-formed steel sections has been performed by the researchers to serve as raw data for calibration of the DSM. The geometry of these various cold-formed steel sections used in experiments has been compiled and named as "pre-qualified columns" and "pre-qualified beams". The geometric limitations for pre-qualified beams and columns are listed in the Appendix 1, Design of Cold-Formed Steel Structural Members using Direct Strength Method (AISI, 2004). As more cross sections are verified for use in the DSM, the pre-qualified geometries requirement will cover more cross sections. Members which do not meet the pre-qualified geometric limits may still use the DSM but with the increased safety factor, Ω and reduced resistance factor, ϕ consistent with any rational analysis method as prescribed in A1.1 of The North American Specification for the Design of Cold-Formed Steel Structural Members (AISI, 2001).

Member capacity prediction using DSM is clear-cut. For local buckling with the potential to interact with flexural, torsional, or torsional-flexural buckling, DSM prediction of the nominal axial strength, P_{nl} for use in cold-formed steel column design is:

$$for\ \lambda_l \leq 0.776 \qquad P_{nl} = P_{ne} \tag{6}$$

$$for\ \lambda_l > 0.776 \qquad P_{nl} = \left[1 - 0.15\left(\frac{P_{crl}}{P_{ne}}\right)^{0.4}\right]\left(\frac{P_{crl}}{P_{ne}}\right)^{0.4} P_{ne} \tag{7}$$

$$where\ \lambda_l = \sqrt{\frac{P_{ne}}{P_{crl}}} \tag{8}$$

The λ_l is local slenderness, P_{crl} is the critical elastic local column buckling load, and P_{ne} is the flexural, torsional, or torsional-flexural buckling strength.

The interaction of distortional and overall buckling is achieved by replacing P_y by P_{ne}. The resulting limiting load P_{nd} is as follows:

$$for\ \lambda_d \leq 0.561 \qquad P_{nd} = P_{ne} \tag{9}$$

$$for\ \lambda_d > 0.561 \qquad P_{nd} = \left[1 - 0.25\left(\frac{P_{crd}}{P_{ne}}\right)^{0.6}\right]\left(\frac{P_{crd}}{P_{ne}}\right)^{0.6} P_{ne} \tag{10}$$

$$where\ \lambda_d = \sqrt{\frac{P_{ne}}{P_{crd}}} \tag{11}$$

The λ_d is distortional slenderness and P_{crd} is the critical elastic distortional column buckling load. The nominal member strength is the lesser of P_{nl} and P_{nd} for compression members.

A comparable set of equations can be derived for the interaction of local and lateral buckling of beams, using a variant of the unified approach for flexural members.

The resulting limiting moment, M_{nl} as given by Equations (12) – (14) accounts for the interaction of local buckling with lateral buckling since the limiting moment is M_{ne} rather than M_y.

$$for\ \lambda_l \leq 0.776 \qquad M_{nl} = M_{ne} \tag{12}$$

$$for\ \lambda_l > 0.776 \qquad M_{nl} = \left[1 - 0.15\left(\frac{M_{crl}}{M_{ne}}\right)^{0.4}\right]\left(\frac{M_{crl}}{M_{ne}}\right)^{0.4} M_{ne} \tag{13}$$

$$where\ \lambda_l = \sqrt{\frac{M_{ne}}{M_{crl}}} \tag{14}$$

The M_{crl} is the critical elastic local buckling moment, and M_{ne} is the nominal flexural strength for lateral-torsional buckling.

The interaction of distortional and lateral buckling of beams can be achieved by replacing M_y by M_{ne}.

$$for\ \lambda_d \leq 0.673 \qquad M_{nd} = M_{ne} \tag{15}$$

$$for\ \lambda_c > 0.673 \qquad M_{nd} = \left[1 - 0.22\left(\frac{M_{crd}}{M_{ne}}\right)^{0.6}\right]\left(\frac{M_{crd}}{M_{ne}}\right)^{0.6} M_{ne} \tag{16}$$

$$where\ \lambda_d = \sqrt{\frac{M_{ne}}{M_{crd}}} \tag{17}$$

The M_{crd} is the critical elastic distortional buckling moment. The nominal member strength is the lesser of M_{nl} and M_{nd} for flexural members.

Since this method uses a computational stability analysis of the cross section, typically a finite strip analysis would be used in determining the strength of open cross sections subject to a variety of different potential instabilities. Finite strip analysis is a general tool that provides accurate elastic buckling solutions with a minimum of effort and time. Thus, a proper cross section stability analysis is able to account for the interaction of the elements of the cross section in an efficient manner, and thus provide a more reliable indicator of true behavior. Yet as mentioned earlier, finite strip

analysis, as implemented in conventional programs, does have limitations. Among them, the two most important ones are:

- The model assumes the ends of the member are simply supported, and
- The cross section may not vary along its length.

The American Iron and Steel Institute has sponsored research that, in part, has led to the development of the freely available program, CUFSM, which employs the finite strip method for elastic buckling determination of any cold-formed steel cross section. Thereafter, for complex sections the calculations are very simple, provided elastic buckling solutions are available.

Advantages of the Direct Strength method of design include everyday design improvements such that there will be no effective properties for strength, no element calculations, no iteration for beams (webs), and that gross properties of the section would be used for strength calculations. In view of the theoretical improvements, the interaction of elements in local buckling (e.g., web/flange interaction) is accounted for, distortional buckling is explicitly treated in the design process, and there is reduction in systematic error in portions of the main Specification.

For applicability and scope, this method is applicable to wider group of cross sections than the main Specification because it provides rational analysis procedure for sections not previously covered thus allows and encourages greater cross section optimization. At this instant numerical methods and rational analysis could be brought to everyday design, and known behavior is integrated into a straightforward design procedure (Schafer, 2006).

The DSM was used extensively throughout this project in order to verify its feasibility to design imported and locally produced cold-formed steel sections in Malaysian construction industry. Besides, experimental results on innovative cold-formed steel sections were compared with the predicted member strength using DSM. If the comparison shows good agreement, proposal would be made for DSM pre-qualified geometry to be extended.

2.6 Remarks to Direct Strength Method

There are a number of limitations of Direct Strength method (DSM) to date. These include: no shear provisions, no web crippling provisions, no provisions for members with holes and limited number/geometry of pre-qualified members, as mentioned beforehand in section 2.5

Moreover, there is no provision for strength increase due to cold-work of forming (Schafer, 2006). As cold-forming of the steel sheet involves work hardening effects, the yield stress, the ultimate strength and ductility are all locally influenced by an amount which depends on the bending radius, the thickness of the sheet and the number of corners. The effect of cold-forming on the yield stress is proven as such:

$$\text{Corner yield stress ratio} = \frac{Corner\ yield\ stress}{Virgin\ yield\ stress} \cong 1.4 \qquad (18)$$

And also, during the cold-forming process varying stretching forces can also induce residual stresses, which can significantly alter the load-bearing resistance of a section. However, DSM does not take into account of the effect of cold-forming thus lead to an over-conservative design of cold-formed steel member.

Rondal (2000) points out that the accuracy of computational models relies largely on the validity of the inputs. Up to now, no agreement has been reached on the distributions and magnitudes to be used for the modelling of residual stresses and geometrical imperfections of cold-formed steel members. This has been mentioned before by Schafer and Peköz (1998).

Residual stresses are stressess that exist in the member as a result of manufacturing and fabricating processes. In cold-formed members residual stresses are dominated by a 'flexural', or through thickness variation. This variation of residual stresses leads to early yielding on the faces of cold-formed steel plates. And also membrane residual stresses cause a direct loss in compressive strength. However analysis of residual stresses (at the integration points of the model for instance) is complex. This vital aspect of the load carrying behavior becomes completely ignored because residual stresses are excluded from the analysis.

Geometric imperfections denote the deviation of a member from 'perfect' geometry. Imperfections of a member include bowing, warping, and twisting as well as local deviations. Local deviations are characterized by dents and regular undulations in the plate. Collected data on geometric sectional imperfections are sorted by Schafer and Peköz (1998) in two categories:

- maximum local imperfection in a stiffened element, and
- maximum deviation from straightness for a lip stiffened or unstiffened flange.

Figure 2.8 shows the two categories of geometric section imperfections.

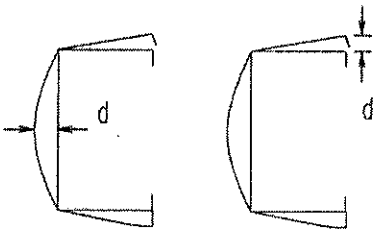

Figure 2.8 Definition of geometric imperfections (Adapted from (Schafer & Peköz, 1998))

Rondal recommended that the collection and analysis of the existing data, with the objective to define guidelines for computational modelling of geometrical imperfections and residual stresses of cold-formed members must be carried out in the future.

Rusch and Lindner (2001) provide observations on the DSM. The DSM is compared to the approaches of effective width, reduced stress and effective thickness. The DSM has assumed the plastic reserve of the section shape to influence the cross section capacity of locally buckled members. In addition, the DSM is unable to distinguish between the support conditions of individual elements of the cross section (e.g. DSM could not be differentiate between four-sided and three-sided supported plates).

Furthermore, the DSM does not consider that interaction between axial force and bending moments. If only an axial force, N is present, the DSM gives the same result as the Effective Width method. But in the cases of bending, the DSM gives different results from the Effective Width method. A closer look is essential for single symmetric sections like U-sections. Local buckling generally causes a shift of the centroid, e_N. If an external axial force N is present, an additional bending moment $M = Ne_N$ occurs. While the Effective Width approach takes this into account, the DSM does not. Thus, the shift leads an overestimation of the load carrying capacity if the DSM is used. Since the DSM does not take into account the additional bending moment and its interaction with axial force, the DSM is not applicable to every type of cross section under axial compression. Thus, user of this method must be alert when designing cross section under axial compression where there is a shift of the centroid.

Besides, in the paper (Rusch & Lindner, 2001) bending tests have been evaluated by using the DSM. It was found that the DSM reflects the ultimate loads reliably though the statistical evaluation reveals that it is not as accurate as the effective width method. In fact, the DSM reflects the behavior in the plastic range, but at higher slenderness, e.g. when the non-dimensional plate slenderness, $\lambda_p \geq 1.1$ the connection with the experimental data is not very fulfilling.

2.7 Column Design Methods

This section introduces the general steps taken in designing thin-walled column (Schafer, 2001):

i. Identify the failure mode/mechanism of interest (e.g. local buckling, distortional buckling or Euler buckling)
ii. Determine the elastic buckling characteristics (e.g. f_{crl}, f_{crd})
iii. Calculate the ultimate strength

For a given failure mode, the elastic buckling stress can be calculated using two methods such as:

i. Element approach, which is a classic solution for buckling of an isolated plate. Equations (19) – (21) show the solution for local buckling of lipped channel and Zed columns. For example, *k=4* is employed for a "stiffened element" assumes it is a simply supported plate in pure compression. Local buckling of the entire member may be predicted by taking the minimum of the connected elements (very conservative approach), alternatively a weighted average may be used, or interaction of elements may be ignored and each element assumed to buckle independently, this is implicitly assumed in the AISI (1996) Specification.

$$(f_{crl})_{web} = k\frac{\pi^2 E}{12(1-\nu^2)}\left(\frac{t}{h}\right)^2 \quad and\ k = 4 \tag{19}$$

$$(f_{crl})_{flange} = k\frac{\pi^2 E}{12(1-\nu^2)}\left(\frac{t}{b}\right)^2 \quad and\ k = 4 \tag{20}$$

$$(f_{crl})_{lip} = k\frac{\pi^2 E}{12(1-\nu^2)}\left(\frac{t}{d}\right)^2 \quad and\ k = 0.43 \tag{21}$$

where h = web depth of lipped channel and zed columns

b = flange width

d = lip length

f_{crl}= local buckling stress

ii. The semi-empirical interaction approach which accounts for local buckling interaction in a single connected element. Equations (22) – (24) show the empirical close-fit solutions for flange/web local buckling and flange/lip local buckling. The modified plate buckling coefficients (i.e., modified k's) account for the influence of a single neighboring element. Local buckling of the entire member may be predicted by taking the minimum of these semiempirical, interaction equations.

$$k_{flange/lip} = -11.07\left(\frac{d}{b}\right)^2 + 3.95\left(\frac{d}{b}\right) + 4 \qquad \left(d/b < 0.6\right) \qquad (22)$$

$$if\ \frac{h}{b} \gg 1 \quad k_{flange/web} = 4\left(\frac{b}{h}\right)^2\left(2 - \left(\frac{t}{h}\right)^{0.4}\right) \qquad (23)$$

$$if\ \frac{h}{b} < 1 \quad k_{flange/web} = 4\left(2 - \left(\frac{h}{b}\right)^{0.2}\right) \qquad (24)$$

where $k_{flange/lip}$ = k value for flange/lip local buckling

$k_{flange/web}$ = k value for flange/web local buckling

For distortional buckling closed-form hand models may be predicted via: current AISI (1996) methods, Lau and Hancock (1987), or Schafer (1997). The AISI (1996) method is based on the work of Desmond (1977). The approaches of Lau and Hancock and Schafer's approach are similar. The Hancock and Schafer models are conceptually the same for the flange, but differ in the methods used to treat the web. Schafer's method explicitly approximates the rotational stiffness at the web/flange juncture in the calculation of the distortional buckling stress. The existing AISI method is unconservative and inaccurate. Simple modifications proposed with an *h/b* correction (the R*AISI method) remove the overall unconservative nature of the prediction, but cannot provide the same level of accuracy as the more robust expressions of Hancock's and Schafer's method.

For the Euler buckling modes for x-axis and y-axis flexural buckling and flexural-torsional buckling the closed-form prediction is given in AISI (1996).

Generally one of the four methods based on the assumptions on the level of interaction between local (L), distortional (D) and Euler (E) modes is considered to determine the stability of the entire cross section.

i. the current AISI approach and small variations, e.g. adding a distortional check,
ii. methods which consider local interaction with long column buckling, but ignore any distortional interactions,

iii. methods which consider local or distortional interaction with long column buckling, and

iv. methods which consider local and distortional interaction as well as local or distortional interaction with long column buckling

In each of the method (i) through (iv) mentioned above, three types of design methods are considered.

i. Effective Width method. Local buckling is considered by finding the portion of an element which is effective in resisting the load at the full applied stress (an element is a part of a member: i.e., the flange, web, lip). Using Winter's curve the strength is determined (similar to AISI in concept, but local buckling is always assumed, for instance the flange of an edge stiffened element always uses $k = 4$, not a modified k). Distortional buckling is considered as either a separate failure mode (member level solution) or compared versus the elastic local buckling stress (element level solution).

ii. Direct Strength method, which uses gross properties of a member to determine the reduced strength of a column in a given mode due to buckling and/or yielding. Local buckling stress (load) is determined for the member as a whole and a local buckling strength is found by using an alternative strength curve. Distortional buckling stress (load) is also determined for the member as a whole and a different strength curve (Hancock's curve) is used. In this solution hand methods are used for all calculations.

iii. Direct Strength method, which is similar to ii, except finite strip solutions are used for the buckling stress (load) in local and distortional buckling instead of hand methods.

Based on the evaluation of design methods performance for lipped C and Z sections, two methods are recommended by Schafer (2000) for thin-walled column design:

i. Effective Width method with L+E and D+E interactions considered

ii. Direct Strength method with L+E and D+E interactions considered

Thorough discussions of the design method performance and explanations on the reasons of choosing these two methods are given in Schafer (2000).

CHAPTER 3
METHODOLOGY

3.1 Introduction to the Work Flow of the Project

The project work scope mainly consists of three major aspects: data gathering, software analysis and experimental work. Figure 3.1 shows a schematic work flow of this project. Firstly, review on literature of cold-formed sections would be carried out. This includes a very broad area such as the overall picture of steel production, import and total consumption in Malaysia, the Effective Width concept and Direct Strength method. All the studies would be assessed and compiled into useful information to be applied in the future. Next, the use of the Effective Width method and Direct Strength method to calculate the nominal design strength of the typical cold-formed steel sections will be studied.

The second part of the project involves member elastic buckling analysis using software. The open source software, CUFSM would be studied in order to analyze the member elastic buckling behaviour and load. After obtaining ample understanding of the software, the cold-formed steel sections would be modeled in CUFSM in order to get the buckling mode and load and subsequently to predict the member strength using Direct Strength Method. At this stage, the cold-formed steel sections manufactured in Malaysia would be highlighted. Further explanation on the usage of CUFSM is demonstrated in section 3.2 and section 3.3

The third part of the project will be experimental work. Experimental testing on selected steel sections available in Malaysia market would be performed and the test results such as buckling mode and load with the member strength calculated at the previous stage. The experimental set up and apparatus are elaborated in section 3.4 in this report.

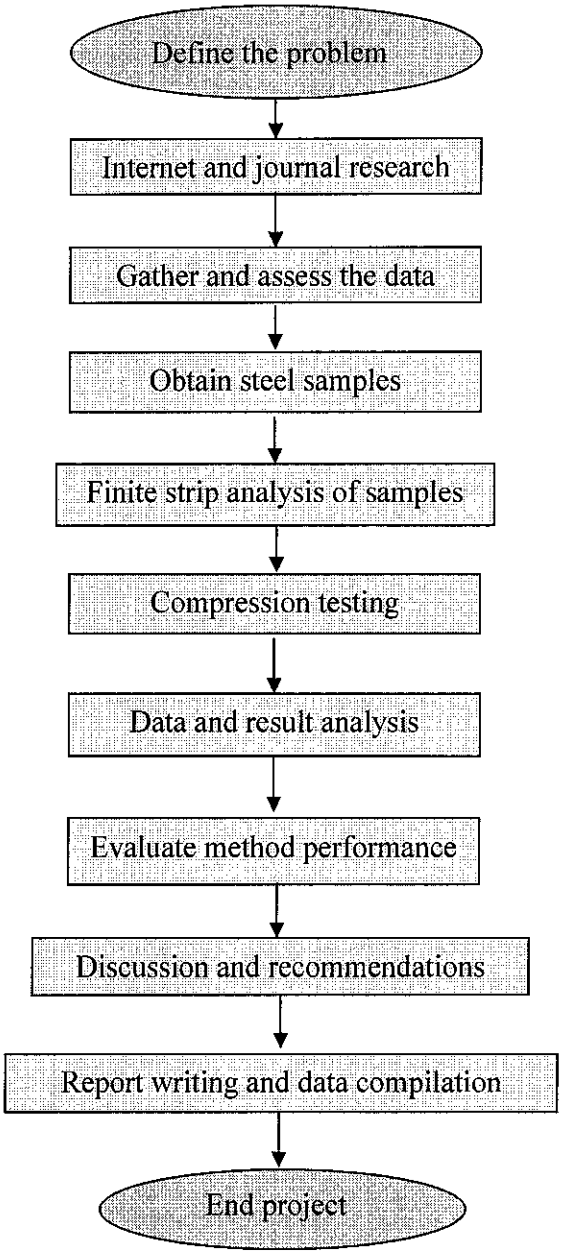

Figure 3.1 Schematic project work flow

3.2 Elastic Buckling Analysis using CUFSM

To aid in the elastic buckling calculation, a freely available program, CUFSM developed by Schafer's research group would be used. This software employs the semi-analytical finite strip method to predict the strength for cold-formed steel members. It examines all the possible instabilities in a cold-formed steel member under longitudinal stresses (axial, bending, or combinations thereof) and thus could identify the buckling mode and load of the members (Schafer & Ádány, 2006). This section discusses the steps to simulate the buckling behavior of cold-formed steel section.

3.2.1 Input

First of all, the material properties of a steel section need to be entered. CUFSM allows the user to define orthotropic materials but this project is using a simple isotropic material. Therefore $E_x = E_y$ and $v_x = v_y$. For instance, for isotropic steel, Young's Modulus E = 200000 N/mm^2, Poisson's ratio v = 0.3, shear modulus of steel G = 76923.08 N/mm^2. If a cross section has multiple material types a new material number could be defined and added to the material properties definition.

Cross section geometry is entered by filling out the nodes and the elements. Elements define how the geometry is connected, how thick the member is, and what material a particular element is composed of. Each node has a "stress" assigned to it. The analysis will give a "buckling load factor" that is a multiplier times the inputted stresses.

Finally, the half-wavelength that the analysis will be based upon will be entered. For local buckling the half-wavelength of interest is close to the maximum dimension of the member. Distortional buckling is usually two (2) to eight (8) times that length, and interest in the longer lengths depends on the application. Figure 3.2 shows the input section of the CUFSM analysis.

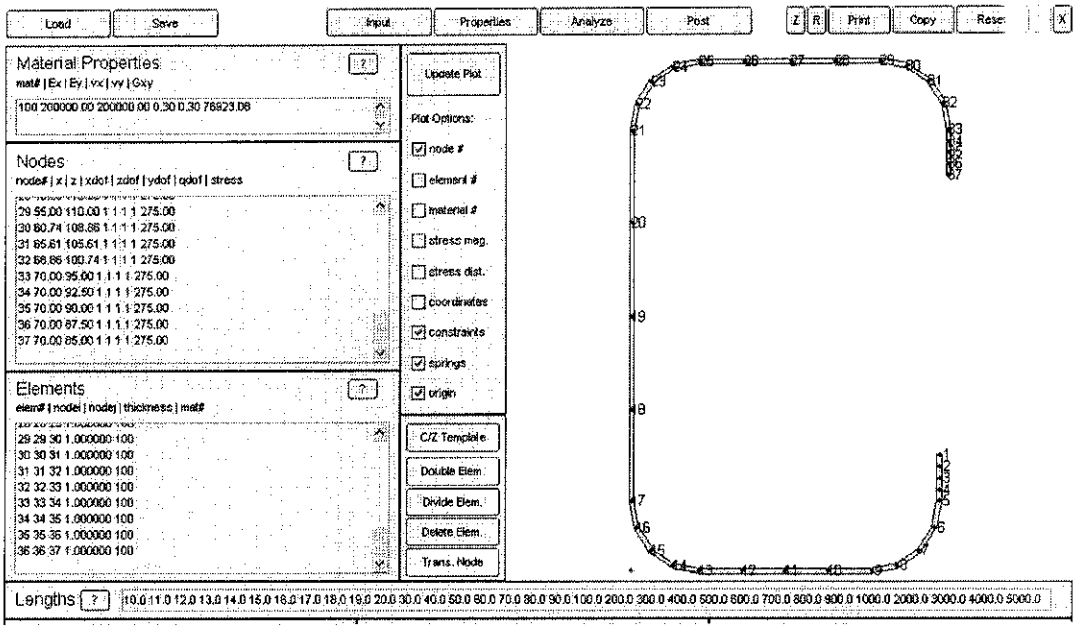

Figure 3.2 "Input" screen of CUFSM analysis

3.2.2 Section Properties, Loads and Moments

The section properties such as cross sectional area, moment of inertia, centre of gravity of relevant axes, origin, etc. are all calculated and shown in this section. The basic properties of cross section are generated by using a straight line model.

Finite strip analysis requires that the user enter in a reference longitudinal stress. The loads are generated based on the f_y the user select. So, the generated P is the squash or yield load, P_y for this section. The M is the moment that causes first yield, M_y etc. Based on the loads the user checks off, a stress distribution is generated. The buckling load factor output is a multiplier times this reference stress.

Figure 3.3 shows the calculated section properties and the calculations of loads and moments for generation of stress on member.

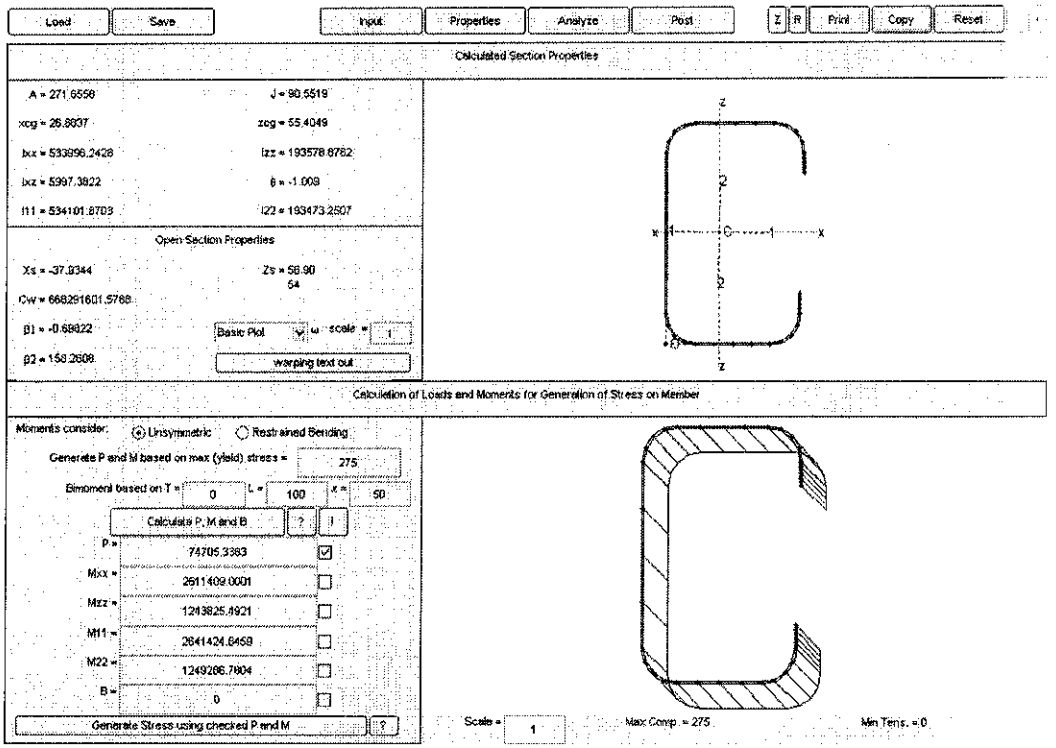

Figure 3.3 "Properties" screen of CUFSM analysis

3.2.3 Output

Figure 3.4 shows what "Post" screen looks like after the user analyze the section. The buckling mode for the first data point is shown above. Different half-wavelengths can be selected using the arrow buttons above and the different mode shapes will be plotted. The minima of the buckling curve identify important locations to examine. The basic concepts such as applied stress, minima, half-wavelength and mode shapes are illustrated in Figure 3.5.

From finite strip analyses local, distortional, and global buckling of a beam and/or column may be identified. The local mode has a strong post buckling reserve and occurs at short half-wavelengths. The distortional mode occurs at intermediate half-wavelengths between local and flexural buckling. The overall mode occurs at longer half-wavelengths and has very little post buckling reserve. From thereon inputs such as elastic buckling load P_{cr} and elastic buckling moment M_{cr} for the Direct Strength method of design can be known.

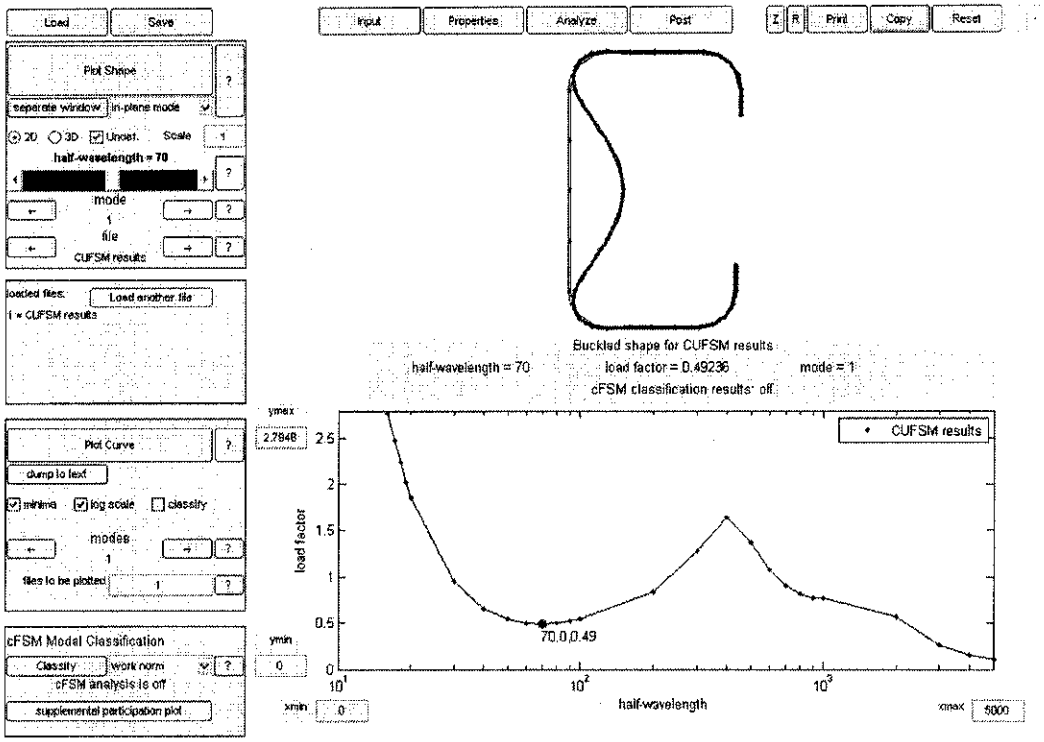

Figure 3.4 "Post" screen of CUFSM analysis

Many buckling modes are revealed at every half-wavelength investigated. Among them the lowest is named as the first mode. Higher modes are those buckling modes at a given half-wavelength that have higher buckling stresses, i.e. higher load or moment than the first mode. Higher buckling modes become more important as bracing and different boundary conditions are considered.

Applied stress on the section indicates that a moment about the major axis is applied to this section. All results are given in reference to this applied stress distribution. Any axial stresses (due to bending, axial load, warping torsional stresses, or any combination thereof) may be considered in the analysis.

Minima indicate the lowest load level at which a particular mode of buckling occurs. The lowest M_{cr}/M_y is sought for each type of buckling. An identified cross-section mode shape can repeat along the physical length of the member.

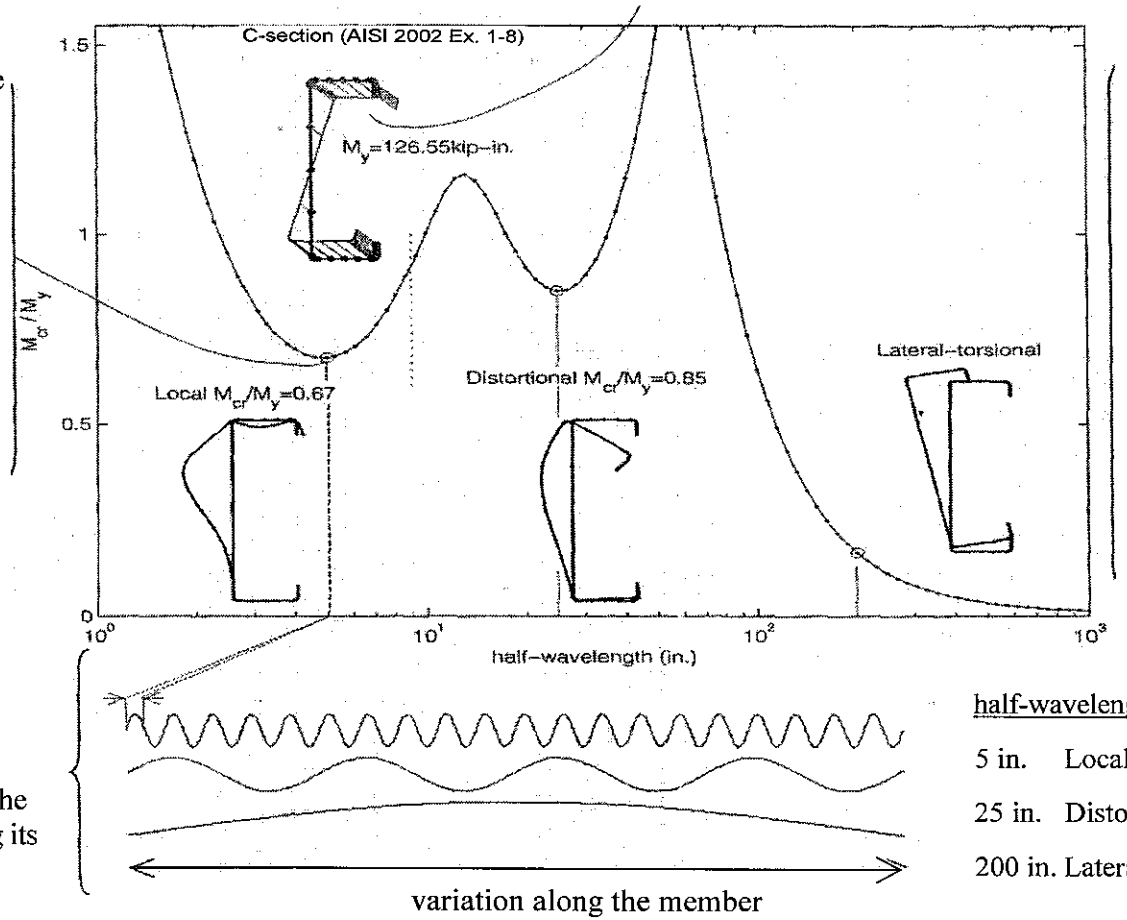

Mode shapes are shown at the identified minima and at 200 in. Identification of the mode shapes is critical to DSM, as each shape uses a different strength curve to connect the elastic buckling results shown here to the actual ultimate strength. In the section, *local* buckling only involves rotation at internal folds, *distortional* buckling involves both rotation and translation of internal fold lines, and *later al-torsional* buckling involves "rigid-body" deformation of the cross-section without distortion.

Half-wavelength shows how a given cross-section mode shape (as shown in the figure) varies along its length.

half-wavelength	
5 in.	Local
25 in.	Distortional
200 in.	Lateral-torsional

Figure 3.5 Understanding finite strip analysis results
(Adapted from Figure 2 DSM Design Guide AISI 2006)

3.3 Elastic Buckling Solutions

The Direct Strength method serves as a useful method to provide elastic buckling solutions. For local buckling, the buckling stress f_{crl} is the minimum point for the local mode on a graph of stress versus half-wavelength as shown at point A in Figure 3.5. The buckling stress could be replaced by a compression load or by a bending moment to simplify the calculations.

For distortional buckling, the buckling stress f_{crd} is the minimum point for the distortional mode on a graph of buckling stress versus half-wavelength as shown at point B in Figure 3.5. The buckling stress could be replaced by a compression load or by a bending moment to simplify the calculations. For complex modes the interaction between the different elements is automatically accounted for (Hancock, Murray, & Ellifritt, 2001).

For the overall modes, the elastic buckling stresses f_e predicted by the formulae in Chapter C of the AISI Specification (2001) are used. This is because the boundary conditions other than simple supports are not considered in the finite strip method. Moreover, moment gradient cannot be accounted for in the finite strip method for flexural members.

3.4 Experiment Setup

A compression test determines the behavior of materials under crushing loads. Column sections will be tested to find out their buckling strength and mode of failure in a compression testing machine. The laboratory testing will be carried out in accordance with the "Standard Test Method for the Compression Testing of Metallic Materials at Room Temperature" (ASTM E 9, 2000) which covers the apparatus, specimens, and procedure for axial load compression testing of metallic materials at room temperature.

The cross sections of column sections are shown in the appendices. Effective cross section properties can be found out using CUFSM software after finding the b/t ratio of each segment as per BS 5950 (BSI, 1987). The test set up is shown in Figure 3.7. Specimen is loaded with both ends between the cross heads of the machine and vertical displacement allowed at one end in loading direction. Specimen is compressed, and deformation at various loads is recorded. The ultimate loads and the nature of failure will be noted.

For the purpose of validation of numerical models, the strain gauges and the dial gauges will be used. The strain gauges will be put at mid height on web and flange portion near the places where the dial gauges are fitted, as shown in Figure 3.6. Compressive stress and strain are calculated and plotted as a stress-strain diagram which is used to determine elastic limit, proportional limit, yield point, yield strength and compressive strength.

Figure 3.5 Location of strain measurement for C-section and Z-section

3.4.1 Apparatus

The apparatus that will be needed to carry out the laboratory testing are as follows:

- Mechanical load frame
- Calibrated force-measuring device (load ring)
- Steel strain gauge
- Dial gauge
- Lever assembly for fitting to dial gauge

Figure 3.7 Compression test set up

3.4.2 Procedure

The procedures to conduct the laboratory testing are delineated in the paragraph below.

A. Preparation of apparatus

1. The load frame is ensured to stand firmly on a solid bench top or support.
2. The attachment of the load ring to the cross-head of the frame is checked and fit any necessary extension pieces, and the upper platen, securely to the lower end of the ring.
3. The load dial gauge is securely held and the end of the stem makes contact with the adjustable stop on the ring. The lower platen is located centrally on the machine platen and the dial gauge post is set vertically upright.
4. The level of the lower platen is adjusted to allow enough clearance to insert the test specimen.

B. Preparation of test specimen

1. Sample steel with preferred cross section and length is prepared.
2. The dimensions of the samples are measured and recorded.

C. Setting up specimen

1. The specimen is placed centrally on the lower platen on the machine, and the specimen axis is checked in vertical.
2. The platen is wind up by hand until the specimen just makes contact with the top platen (this is indicated by a fractional movement of the load dial gauge).
3. The strain dial gauge is adjusted on the pillar to read zero, or a convenient initial reading.

D. Compression test

1. The motor is switched on and the load is applied.
2. The readings are recorded at regular intervals every 0.1 *kN/sec*.
3. Loading is continued and the readings are taken until it is certain that failure has occurred.
4. The machine is stopped when the specimen has failed, the motor is allowed to stop completely and put into reverse.

E. Sketching mode of failure

1. The failure of specimen is looked at carefully.
2. The photograph of the specimen is taken after failure to indicate the manner in which it failed and especially to which of the three main types of failure it belongs: local, distortional and global buckling.

F. Removing specimen

1. The machine is stopped when the specimen has failed, allow it to stop completely and it is put into reverse, or wind down until the load is taken off the specimen.
2. The strain dial gauge is read as a check on the initial reading under zero load.
3. The machine plate is lowered far enough to enable the specimen to be removed.

3.5 Hazard Analysis

This section analyzes the hazards that exist when the project is being carried out. "Hazard" refers to anything that can cause harm (e.g. chemical, electricity, working from ladders, etc.). The conclusion of hazard identification should result in a list of hazard sources, the particular form in which that hazard occurs and the areas of workplace or work process where it occurs.

A hazard check list has been developed through the author's observation and consultation with technicians. After analyzing the work process, the hazards that might be experienced by the author are ergonomics risk and Musculoskeletal Disorders. This is because the author would spend lengthy time running the simulation of cold-formed steel buckling using the computer software. As such, the author might suffer from backache, eye strain, injuries of muscles and discomfort due to repetitive hand movement and awkward posture.

There are a wide variety of possible solutions that can be implemented to reduce or eliminate the ergonomic risk associated with this project work process in the workplace. First of all, a comprehensive reading of work-related musculoskeletal disorders of the neck, upper extremity, and low back and exposure to physical factors at work would be studied. Since the author will be using computer at a high regularity, the author will create a safe and comfortable computer workstation applying simple principles offered by OSHA (Occupational Safety and Health Administration). The author will adopt a "correct" posture and a custom-fit arrangement of components. When setting up a computer workstation or performing computer-related tasks, the author will ensure the checklist is being followed (see Appendix A). Herein, several matters are also noteworthy:

- computer cables are shielded with a split wire loom, a flexible and durable polyethylene corrugated tube with a split down the side
- cables, power adapters, power strips, hubs, modems and other small devices are readily lifted off the floor and put safely out of harm's way with cable management products that loop

- with a glut of equipment, wiring and electrical outlets conducting heat, often over long periods of time and in compact spaces, fire safety is an important workspace consideration thus fire safety measures would be employed.

The second potential hazard that the author might experience is physical accident while carrying out experiment in the structural laboratory. Since the experiment will involve performing compression test on cold-formed steel sections, the author will be exposed to physical danger such as cuts, impact and blow when operating the compression machine. The most common laboratory accident is probably the cut received while attempting to apply force on the cold-formed steel sections.

In order to prevent the physical danger in laboratory, several actions will be taken. Firstly, the author would try to wrap the sharp edge of machine and cold-formed steel sections with a heavy-duty duct tape to protect the author from accidental laceration. This is especially important before placing the section on the machine. Professional standards of personal behavior are required too:

- Use laboratory equipment only for its designated purpose
- Do not allow visitors in laboratories where hazardous activities are in progress.
- Confine long hair and loose clothing in the laboratory. Wear shoes at all times.
- Keep work areas clean and free from obstruction.
- Do not block access to exits, emergency equipment, controls, and electrical panels.

In conclusion, the purpose of this hazard analysis is to remind the author on the principal workstation hazards that should be controlled in order to prevent accidents and work related disease. It is important to create a comfortable working environment so that the author feel less exhausted and stressed in places where the author has to spend long hours. Creation of a comfortable working environment is also believed, will enable the author to put her abilities to use more effectively and revitalize workplaces.

CHAPTER 4
RESULTS AND DISCUSSIONS

4.1 Introduction

In this section, the results of this study are reported and discussed. The results that are presented consist of:

- comparison of the ultimate load reported in literature with that predicted using DSM
- comparison of the ultimate load of the laboratory testing with that predicted using DSM

Besides, the difficulties arose when performing the compression test as well as the recommendations to overcome the difficulties are presented.

4.2 Comparison of the Ultimate Load Reported in Literature with that Predicted using DSM

The experimental results reported in literature are compared with the ultimate load calculated using DSM. A brief clarification on the experiment testing in literature and a discussion on the comparison are included.

4.2.1 Compression Test on C-section by Mahmood et al. (2005)

A pure compression test on C-section was carried out by Mahmood et al. (2005). The C-section dimension is shown in Figure 4.1. A detailed dimension of the section is attached in Appendix B. The geometrical configuration of the section is manufactured by Tong Yong Private Limited with the uniform thickness of 1 mm for C-section. The design strength of the material is expected to have the average yield strength of 275 N/mm^2 based on the coupon test conducted.

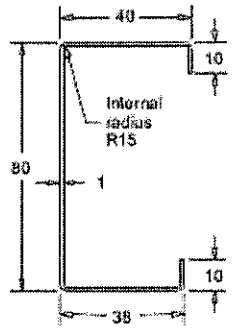

Figure 4.1 80x40x38 C-section based on Mahmood et al. (2005)

The laboratory testing of the C-section was carried out in accordance with the code of practice. Short strut, which is defined as a 500 mm long specimen was tested for local buckling capacity. The short strut specimen represents the capacity of the sections which failed due to local buckling. Long strut with the length of 1000 mm long was tested for the combination of local and overall bucking capacity.

Both analytical and experimental approaches were carried out in the study of Mahmood et al. (2005). The method of analyzing the strength of the cold-formed was based on BS5950- Part 5:1987.

To evaluate the proposed Direct Strength method for the design of cold-formed steel section, the capacity of the 500 mm and 1000 mm long C-section was predicted based on Direct Strength method and was compared with the test value and Effective Width method.

4.2.1.1 CUFSM Analysis Results

The C80x40x38 section was evaluated using CUFSM as in Appendix B. The result shows that under pure compression, the C-section serving as a column has a few important cross section stability elastic buckling modes:

- Local buckling which occurs at a stress of 159.5 N/mm^2 and may repeat along the length of a member every 60.1 mm (it is the half-wavelength)
- Distortional buckling which occurs at a stress of 255.75 N/mm^2 and may repeat along the length of a member every 326.2 mm (it is the half-wavelength)

- Global flexural buckling, which for a 500 mm long member occurs at a stress of 954.25 N/mm^2
- Global flexural buckling, which for a 1000 mm long member occurs at a stress of 245.40 N/mm^2

The finite strip analysis and a column chart developed for C80x40x38 section are presented in Appendix B.

4.2.1.2 Comparison with Test Result

The test result of compression test on the C-section is in accordance with the theoretical values derived from the British code of practice and AISI (2004). The summary of the comparison of results between the theoretical values and experimental values is tabulated in Table 4.1.

Table 4.1 Comparison of ultimate loads for C80x40x38

Specimen	Length (mm)	Capacities (kN)			Test-to-predicted ratio	
		Test Value	EWM in BS 5950-5:1987	DSM in AISI (2004)	EWM in BS 5950-5:1987	DSM in AISI (2004)
C80x40x38	500	38	33.70	33.60	1.128	1.131
C80x40x38	1000	25	22.84	24.78	1.095	1.009

* EWM= Effective Width method

From the table, for 500 mm short strut, it is found that the test-to-predicted ratio is 1.128 and 1.131 for Effective Width method and DSM respectively. Both methods are considered conservative. Similarly, for 1000 mm slender strut test value is 1.095 and 1.009 for Effective Width method and DSM respectively, which are good and acceptable. The comparison shows that for intermediate column DSM is a slightly better method than the BS Effective Width method for this C-section whereas for short strut Effective Width method better predicts the ultimate load.

4.2.2 Compression Test on Innovative Cold-formed Steel Columns by Narayanan et al. (2003)

Laboratory experiments were carried out by S. Narayanan and M. Mahendran on 16 innovative 1000 mm long steel column under axial compression. The steel column sections were placed between the cross-heads of a compression testing machine and loaded to failure. The ultimate design load capacities were evaluated using the provisions of Australian Cold-formed Steel Structures Standard AS/NZS 4600-1996 and were compared with those from experiments and finite element analyses.

Five sections, namely Column 1, Column 2, Column 6, Column 7 and Column 15, were chosen from among the 16 to carry out the comparison between the experimental value and calculated strength based on DSM. Figure 4.2 shows the cross section of the innovative sections. Column 1 was also tested in a series of different lengths (876 mm, 675 mm, 475 mm, 275 mm, 130 mm, and 100 mm) thus comparison was also made. The properties of all the innovative steel columns are shown in Appendix C.

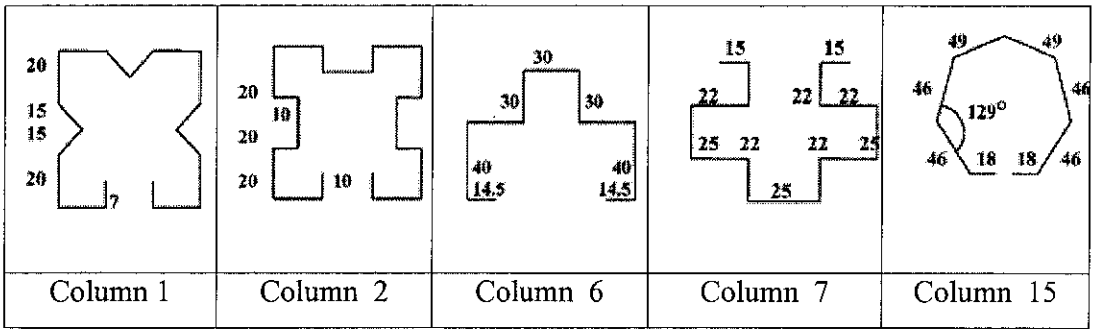

Figure 4.2 Innovative column sections

To evaluate the proposed Direct Strength method for the design of cold-formed steel section, the capacity of the innovative sections was predicted based on Direct Strength method in AISI (2004) and was compared with the test value and that computed using AS/NZS 4600.

4.2.2.1 CUFSM Analysis Results

All the five steel sections were evaluated using CUFSM, as shown in Appendix C. Table 4.2 shows that under pure compression, each innovative section serving as a column has a few important cross section stability elastic buckling modes.

It is shown that local buckling for Column 1, 2, and 15 occurs at a half-wavelength less than the largest characteristic dimension of the section except for Column 6 and 7. Distortional buckling for Column 15 occurs at a half-wavelength roughly 30 times greater than the largest section dimension. As the member length is 1000 mm thus the interest for global buckling is focused at a half-wavelength of 1000 mm.

Table 4.2 Buckling behaviour for innovative cold-formed steel columns

Column	Local buckling		Distortional buckling		Global flexural buckling	
	Load (kN)	Half-wavelength (mm)	Load (kN)	Half-wavelength (mm)	Load (kN)	Half-wavelength (mm)
1	292.88	20	151.96	200	52.75	1000
2	245.78	20	284.88	200	59.14	1000
6	354.99	180	169.84	350	50.45	1000
7	186.88	35	344.56	200	62.91	1000
15	169.83	50	83.81	1400	299.7	1000

The finite strip analysis and calculation are presented in Appendix C.

4.2.2.2 Comparison with Test Result

The comparison of results between theoretical values and experimental values for the five (5) innovative cold-formed steel sections is tabulated in Table 4.3.

Table 4.3 Comparison of ultimate loads for the innovative cold-formed steel sections

Specimen	Capacities (kN)			Test-to-predicted ratio	
	Test Value	AS/NZS 4600	DSM in AISI (2004)	AS/NZS 4600	DSM in AISI (2004)
Column 1	78.0	80.6	52.7	0.968	1.480
Column 2	86.0	89.7	51.9	0.959	1.657
Column 6	80.1	105.8	44.2	0.757	1.812
Column 7	104.5	117.2	55.2	0.892	1.893
Column 15	83.1	92.8	69.3	0.895	1.199

The experimental value is very much higher than the theoretical value of DSM whereby the test-to-predicted ratio ranges from 1.199 to 1.893. DSM underestimates the capacity of the innovative cold-formed columns. This is understandable because the geometry of the innovative sections falls outside the "pre-qualified" columns of DSM 1.1.1.1. AS/NZS 4600 is a better prediction method than DSM. Further research is needed to improve the accuracy of DSM predictions for buckling strengths of innovative cold-formed steel columns made of thin, high-strength steels.

The comparison of buckling modes and ultimate loads for different lengths of Column 1 is tabulated in Table 4.4.

Table 4.4 Comparison of buckling modes and ultimate loads for different lengths of Column 1

Column length (mm)	Test		DSM in AISI (2004)		Test-to-predicted ratio
	Capacities (kN)	Buckling mode	Capacities (kN)	Buckling mode	
100	123.6	Local	104.5	Distortional	1.183
130	122	Local	98.1	Distortional	1.244
275	107.2	Distortional	93.8	Distortional	1.142
475	102.1	Distortional	93.8	Distortional	1.088
675	90.9	Distortional	81.0	Distortional	1.122
876	87.6	Distortional	63.3	Local/Flexural	1.385
1000	78	Distortional	52.7	Local/Flexural	1.479

From the table, it is found that the experimental value is very much higher than the theoretical value of DSM. The predicted buckling mode also differs than the test failure mode. For length of 876 mm and 1000 mm, the local-global interaction was strong and must be included in DSM however in real testing the column failed in distortional buckling. Since the geometry of all the innovative sections falls outside the "pre-qualified" columns of DSM 1.1.1.1 the ultimate strength of the sections could not be evaluated using DSM.

4.3 Comparison of the Ultimate Load of the Laboratory Testing with that Predicted Using DSM and BS Effective Width Method

A series of pure compression tests were carried out on the samples being manufactured by BlueScope Lysaght Malaysia Sdn. Bhd. The sections are C-section namely C15015, C15019 and Z-section namely Z15015, Z15019. Figure 4.3 shows the geometry configuration of Lysaght C-section and Lysaght Z-section.

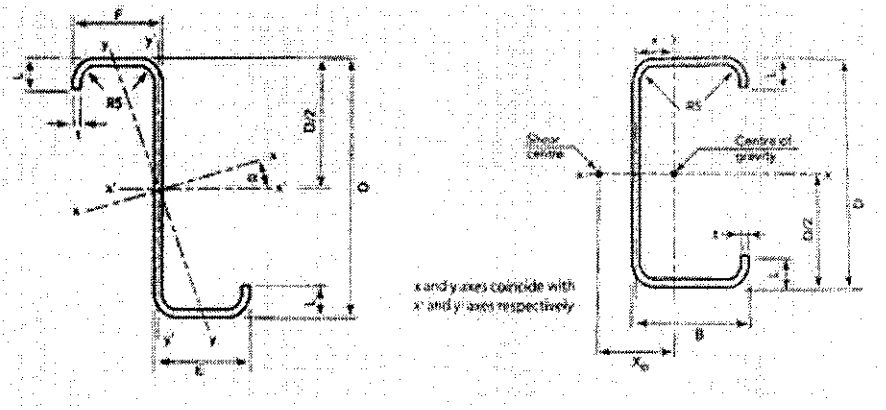

Figure 4.3 (a) Lysaght Z-section (b) Lysaght C-section

Lysaght C-sections have equal flanges and are suitable for simply supported spans. For shorter spans they may be used continuously over two or more spans with ends butted, thus producing reduced deflection compared with simple spans. They cannot be lapped. Lysaght Z- sections feature one broad and one narrow flange, sized so that two sections of the same size fit together snugly, making them suitable for lapping. The design strength of the material is expected to have the average yield strength of 450 N/mm^2 based on the mill certificates provided by the company. The cross sections and properties of the steel columns are shown in Appendix D.

Both experimental and analytical approaches were carried out in the study. Experimental work involved testing of the individual capacities of the C-section and Z-section for compression. Each section was tested in length of 500 mm and 1000 mm. The steel column sections were placed between the cross-heads of a compression testing machine and loaded to failure. The testing procedures are prescribed in Section 3.4. The method of analyzing the strength of the cold-formed was based on BS5950: Part 5:1998, Eurocode 3 Part 1.3 (CEN, ENV 1993-1-3) and Direct Strength Method (AISI, 2004). Subsequently, comparison was made with the test values from experiments. The calculations using Effective Width method of both design codes are shown in Appendix D.

4.3.1 CUFSM Analysis Results

All the C-sections and Zed-sections were evaluated using CUFSM. The the finite strip analysis and calculation are presented in Appendix D. Table 4.2 shows that under pure compression, each innovative section serving as a column has a few important cross section stability elastic buckling modes. Due to the miniature difference in the cross section dimension, the elastic buckling modes and half-wavelengths are different for the same section with different length.

Table 4.5 Buckling behavior of the test specimens

Specimen	Length (mm)	Local buckling		Distortional buckling		Global flexural buckling	
		Load (kN)	Half-wavelength (mm)	Load (kN)	Half-wavelength (mm)	Load (kN)	Half-wavelength (mm)
C15015	500	48.64	114.3	81.60	426.1	1365.59	500
	1000	50.99	112.0	83.99	504.0	349.91	1000
C15019	500	96.59	111.4	133.70	501.1	1718.16	500
	1000	94.78	111.6	130.24	502.1	418.95	1000
Z15015	500	49.07	110.5	83.92	600.0	1261.49	500
	1000	48.57	110.5	84.99	600.0	254.23	1000
Z15019	500	80.24	111.2	121.02	500.0	1501.30	500
	1000	97.65	111.0	141.23	499.2	402.08	1000

4.3.2 Analysis of test results

The load-displacement relationships for all the specimens obtained through the tests are shown in Appendix D. One of the graphs is illustrated in Figure 4.4. The maximum load recorded on the graph is considered as the ultimate load of the specimen.

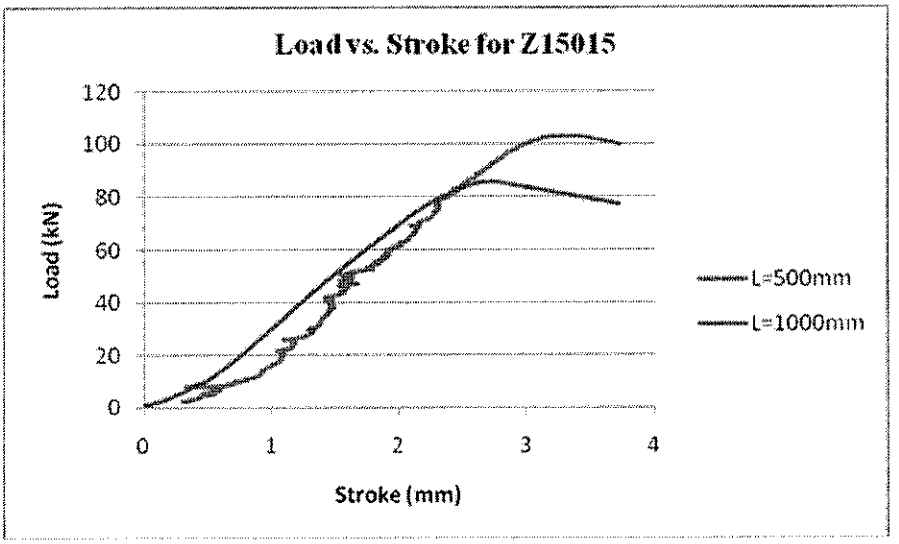

Figure 4.4 Graph of load vs. stroke for specimen Z15015

It is seen that the ultimate load for the specimen of 500 mm length is higher than that of 1000 mm. This is expected because the long strut deformed earlier under the interaction of local and global buckling effect due to longer compression length. So generally the ultimate load of shorter length specimen is higher. However Table 4.6 shows that for C15015, C15019 and Z15019, the ultimate load for the 500 mm length specimen is lower than that of 1000 mm length specimen. This signifies that there must be some error involved in the compression tests.

Due to the loading condition of the member and uneven end surface of the section, part of the section that curved out would support more load than the other elements. This resulted in an early buckling of elements than was anticipated. Thus, the member strength could not be developed fully and the ultimate load is lower than the expected value especially for 500 mm length specimen.

Table 4.6 shows the buckling mode of all specimens. In decision of buckling mode, at early stage of the compression test, flange buckling occurred followed by flange/lip junction. After that, web local buckling developed and flange/web junction deformed slightly. Finally the sections deformed in distortional mode. All the specimens failed due to interaction of distortional and global buckling at the mid height of member, or by member end buckling, i.e. the web distortional buckling.

Figure 4.5 shows the formation sequence of buckling mode for Z15015 throughout the compression test. The pictures of section deformation and failure mode of all specimens are shown in Appendix D.

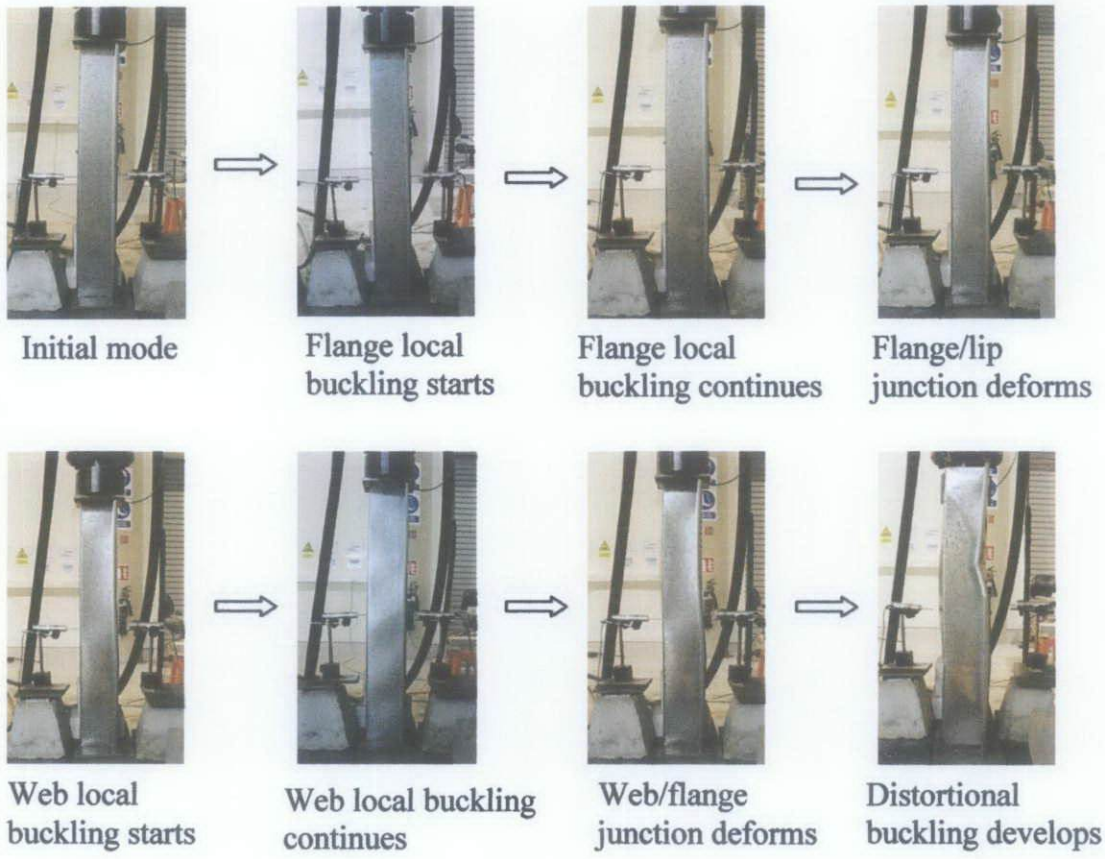

Figure 4.5 Formation sequence of buckling mode for Z15015

4.3.3 Comparison with Test Result

The summary of the comparison of results between theoretical values and experimental values for the specimens is tabulated in Table 4.6.

A good congruence was generally found between the values obtained through the Effective Width method in BS5950-5:1998 and the test value, particularly in test-to-predicted ratio of 1.002 and 0.847 for C-section and Z-section respectively.

When compared with results obtained via the DSM, differences obtained were greater. The mean test-to-predicted ratio for tests on C-sections is 0.906 whereas for Z-sections is 0.978.

The greatest difference between theoretical and experimental value turned out for the Effective Width method in Eurocode 3 Part 1.3 (CEN, ENV 1993-1-3). The mean test-to-predicted ratio for C-sections is 1.045 while for Z-sections is 1.244.

From the table, it is found that most of the experimental value is lower than the predicted value. As mentioned beforehand in the analysis of data, this phenomenon indicates that:

- The compression test requires adjustments to promote buckling at the mid-height of the testing specimen
- The prediction methods require revision because the methods over-predict the ultimate loads for certain sections

Interaction of distortional buckling and global buckling is more prevalent in the experimental data on C-sections and Zed-sections. This shows a good agreement with the buckling modes analyzed using the finite strip analysis.

Table 4.6 Comparison of ultimate loads for Lysaght C-sections and Z-sections

Column	Length (mm)	Capacities (kN)				Buckling mode		Test-to-predicted ratio		
		Test	DSM in AISI (2004)	Effective Width method in BS5950-5:1998	Effective Width method in Eurocode 3	Test	DSM in AISI (2004)	DSM in AISI (2004)	Effective Width method in BS5950-5:1998	Effective Width method in Eurocode 3
C15015	500	82.83	99.57	85.89	95.91	D+G*	D+G	0.832	0.964	0.864
	1000	98.40	91.57	82.39	72.48	D+G	D+G	1.075	1.194	1.358
C15019	500	110.52	141.74	126.05	137.60	D+G	D+G	0.780	0.877	0.803
	1000	117.31	124.90	120.67	101.63	D+G	D+G	0.939	0.972	1.154
Z15015	500	102.93	108.86	114.27	93.78	D+G	D+G	0.946	0.901	1.098
	1000	85.62	91.08	104.95	64.42	D+G	L+G**	0.940	0.816	1.329
Z15019	500	127.32	138.03	168.44	131.91	D+G	D+G	0.922	0.756	0.965
	1000	140.30	127.28	153.30	88.52	D+G	D+G	1.102	0.915	1.585

* D+G= Interaction of distortional buckling and global buckling
** L+G= Interaction of local buckling and global buckling

4.4 Problems and Precautions when Performing Compression Test

There were some difficulties arose when performing the compression tests on the steel specimens at the university laboratory. Firstly, the steel strain gauge which is to measure the strain of specimens was unavailable. Due to the financial constraint, the less expensive steel strain gauge was purchased. Unlike the more expensive strain gauge, the wiring and soldering of the purchased strain gauge must be made manually thus affected the sensitivity of the items. To overcome this problem, an early purchase order shall be made in advance to the laboratory executive to ensure that the better strain gauge is purchased.

Secondly, the tested specimens deformed at loads very much lower than the predicted compression capacity due to the uneven end surface of specimen, as shown in Figure 4.6. Due to the imprecise member cutting during the cold-rolling process the end surface of the specimen is very rough and not perpendicular to the longitudinal axis of the specimen. Efforts were done to improve the condition however there was slim gap between the loading plate and the specimen end.

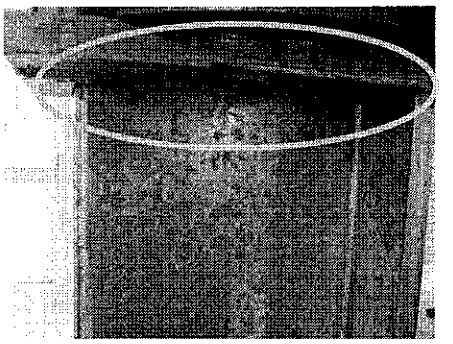

Figure 4.6 Uneven end surface of specimen

Besides, to have pure compression load acting on the specimen, i.e. no eccentricity, the specimen centroid must be aligned with the centroid of the loading plate. Since it was difficult to locate precisely the centroid of specimen, error might arise due to the eccentricity of loading which led to bending effect.

CHAPTER 5
CONCLUSIONS AND RECOMMENDATIONS

Cold-formed steel has become a competitive building material in the last two decades because of its unique characteristics and advantages. However, to ensure sustained market growth for the cold-formed steel in building construction, design method must be enhanced. A Direct Strength method is proposed for cold-formed steel member design considering the behavior of local, distortional and Euler buckling. The method uses separate column curves for local buckling and distortional buckling, with the slenderness and maximum capacity in each mode controlled by consideration of Euler buckling. This method offers many advantages over current Effective Width method.

This project presents the comparison of the ultimate strength of cold-formed steel compression member obtained based on the test value and the applications of BS 5950-5 standard, the recently developed ENV-1993-1-3 and Direct Strength method in AISI (2004). The conclusions can be drawn as follows:

(1) The mean test-to-predicted values for C-section 80 x 40 x 38 for BS and DSM predictions were 1.112 and 1.070 respectively and acceptable. These are "pre-qualified" sections.

(2) The ultimate strength of innovative column sections cannot be predicted using DSM because these are not "pre-qualified" sections. New predictor equations have to be determined.

(3) The test-to-predicted values for the Lysaght C-sections and Z-sections for BS predictions varied between 0.756 and 1.194 with the mean equals to 0.924. For DSM predictions the values varied between 0.780 and 1.102 with the mean equals to 0.942. DSM yields reasonable and better strength predictions. These are also "pre-qualified sections".

Based on the study, it is recommended to apply DSM in local industry because it offers many advantages over the current method. However, further exploration shall be continued in order to develop the DSM. This includes the following:

(1) More laboratory test shall be carried out on locally produced cold-formed steel to compare the test results with the ultimate strength calculated using the Direct Strength method and Effective Width method. This is necessary to verify the method and also to expand the "pre-qualified" sections database.
(2) The guidelines on using the Direct Strength method in local industry must be reviewed to enhance its recognition and practice among local steel designers.
(3) The local acceptance of the use of cold-formed steel would be compared to hot-rolled steel and concrete to encourage the use of cold-formed steel in Malaysians construction industry.

Throughout the study, the author has gained valuable understanding on the failure modes and compression capacities of cold-formed steel by using the various prediction methods and by performing the compression test on locally produced cold-formed steel sections.

REFERENCES

AISC. (1993). *Load and Resistance Factor Design Specification for Structural Steel Buildings, 1993.* American Institute of Steel Construction.

AISI. (2001). *North American Specification for the Design of Cold-Formed Steel Structural Members.* Washington, D.C., AISI/COS/NASPEC 2001: American Iron and Steel Institution.

AISI. (1996). *Specification for the Design of Cold-Formed Steel Structural Members.* Washington: American Iron and Steel Institute.

AISI. (2004). *Supplement 2004 to the North American Specification for the Design of Cold-Formed Steel Structural Members, 2001 Edition: Appendix 1, Design of Cold-Formed Steel Structural Members Using Direct Strength Method.* Washington, D.C., SG05-1: American Iron and Steel Institute.

AS/NZS. (1996). *Cold Formed Steel Structures, AS/NZS 4600:1996.* Standards Australia/Standards New Zealand.

ASTM E9-89a. Standard Test Methods of Compression Testing of Metallic Materials at Room Temperature. In 2000.

BSI. (1987). *British Standard: Structural Use of Steelwork in Building, Part 5. Code of Practice for the Design of Cold-Formed Sections.* London: British Standards Institution BS5950 Part 5:1987.

Cheung, Y. K., & Tham, L. G. (1998). The Finite Strip Method. *CRC Press.*

Chodraui, G. M., Neto, J. M., Gonçalves, R. M., & Malite, a. M. (2006). Distortional Buckling of Cold-Formed Steel Members. *Journal of Structural Engineering , 132* (4).

Hancock, G. J. (2003). Cold-Formed Steel Structures. *J. of Constructional Steel Research, Elsevier. 59(4)* , 473-487.

Hancock, G. J., & Lau, S. C. (1987). Distortional Buckling Formulas for Channel Columns. *Journal of Structural Engineering,ASCE,1987, 113(5)* , 1063 – 1078.

Hancock, G. J., Kwon, Y. B., & Bernard, E. (1994). Strength Design Curves for Thin-Walled Sections Undergoing Distortional Buckling. *J. Constr. Steel Res. , Vol. 31, Nos. 2/3*, 169-186.

Hancock, G. J., Murray, T. M., & Ellifritt, D. S. (2001). *Cold-Formed Steel Structures to the AISI Specification.* New York: Marcel Dekker.

Newman, A. (1997). *Metal Building Systems Design and Specifications.* New York: McGraw-Hill.

Rhodes, J., & Harvey, J. M. (1977). Interaction Behaviour of Plain Channel Columns under Concentric or Eccentric Loading. *Proc 2nd Int Colloquium on the Stability of Steel Struct., ECCS, Liege*, (pp. 439-44).

Rondal, J. (2000). Cold Formed Steel Members and Structures- General Report. *J Const Steel Res 55 1-3* , 155-158.

Rusch, A., & Lindner, J. (2001). Remarks to the Direct Strength Method. *Thin Wall Struct 2001 , 39(9)*, 807-20.

S., N., & M., M. (2003). Ultimate capacity of innovative cold-formed steel columns. *Journal of Constructional Steel Research 59* , 489-508.

Schafer, B. W. (1997). *Cold-Formed Steel Behavior and Design: Analytical and Numerical Modeling of Elements.* Ph.D. Thesis. Cornell University. Ithaca, New York.

Schafer, B. W. *Cross section Stability of Structural Steel.*

Schafer, B. W. (2006). Designing Cold-Formed Steel using the Direct Strength Method. *18th International Specialty Conference on Cold-Formed Steel Structures.* Orlando, FL. October 2006.

Schafer, B. W. (2000). *Distortional Buckling of Cold-Formed Steel Columns.* Final Report to the American Iron and Steel Institute (AISI).

Schafer, B. W. (2002). Local, Distortional, and Euler Buckling in Thin-Walled Columns. *J. of Structural Engineering, ASCE* , 128(3) 289-299.

Schafer, B. W. (2008). Review: The Direct Strength Method of cold-formed steel member design. *Journal of Constructional Steel Research , 64*, 766–778.

Schafer, B. W. (2001). Thin-Walled Column Design Considering Local, Distortional, and Euler Buckling. *Proceedings of the Structural Stability Research Council.*

Schafer, B. W., & Ádány, S. (2006). Buckling Analysis of Cold-Formed Steel Members using CUFSM: Conventional and Constrained Finite Strip Methods. *18th International Specialty Conference on Cold-Formed Steel Structures.* Orlando, FL. October 2006.

Schafer, B. W., & Ádány, S. (2005). Understanding and Classifying Local, Distortional and Global Buckling in Open Thin-Walled Members. *Annual Conference, Structural Stability Research Council.* Montreal, Canada.

Schafer, B. W., & Peköz, T. (1998). Computational Modeling of Cold-Formed Steel: Characterizing Geometric Imperfections and Residual Stresses. *J. of Const. Steel Research. Elsevier , 47(3).*

Schafer, B. W., & Peköz, T. (1998(b)). Direct Strength Prediction of Cold-Formed Steel Members Using Numerical Elastic Buckling Solutions. *Thin-Walled Structures, Research and Development, Eds. Shanmugan, N.E., Liew, J.Y.R., and Thevendran, V., Elsevier* , 137-144.

Schafer, B., & Adany, S. (2006). *Buckling analysis of cold-formed steel members.* 18th International Speciality Conference.

Tahir, M. M., Tan, C. S., & Shek, P. N. (2006). Typical Tests on Cold-Formed Steel Structures. *6th APSEC 2006.* KL, Malaysia.

Tahir, M. M., Thong, C. M., & Tan, C. S. (2005). Performance of Locally Produced Cold-Formed Steel Sections for Roof Truss System. *Jurnal Teknologi Vol 42(B) June* , 11-28.

Von Karman, T., Sechler, E. E., & Donnell, L. H. (1932). The Strength of Thin Plates in Compression. *transactions ASME , Vol. 54*, MP 54-5.

Wegrzyn, J. E., Mahajan, D., & Gurevich, M. (1999). Catalytic routes to transportation fuels utilizing natural gas hydrates. *Catalyst Today , Volume 50* (Issue 1), Pages 97-108.

Young, B., & Rasmussen, K. (1999). Behaviour of Cold-Formed Singly Symmetric Columns. *Thin Wall Struct , 33(2)*, 83-102.

Yu, W.-W. (2000). *Cold-Formed Steel Design* (3rd ed.). WILEY-IEEE.

APPENDIX A

OSHA ERGONOMIC EVALUATION CHECKLIST ON COMPUTER WORKSTATION

Evaluation Checklist

WORKING POSTURES–The workstation is designed or arranged for doing computer tasks so it allows your	Y	N
1. **Head** and **neck** to be upright, or in-line with the torso (not bent down/back). If "no" refer to Monitors, Chairs and Work Surfaces.		
2. **Head, neck,** and **trunk to** face forward (not twisted). If "no" refer to Monitors or Chairs.		
3. **Trunk** to be perpendicular to floor (may lean back into backrest but not forward). If "no" refer to Chairs or Monitors.		
4. **Shoulders** and **upper arms** to be in-line with the torso, generally about perpendicular to the floor and relaxed (not elevated or stretched forward). If "no" refer to Chairs.		
5. **Upper arms** and **elbows** to be close to the body (not extended outward). If "no" refer to Chairs, Work Surfaces, Keyboards, and Pointers.		
6. **Forearms, wrists,** and **hands** to be straight and in-line (forearm at about 90 degrees to the upper arm). If "no" refer to Chairs, Keyboards, Pointers.		
7. **Wrists** and **hands** to be straight (not bent up/down or sideways toward the little finger). If "no" refer to Keyboards, or Pointers		
8. **Thighs** to be parallel to the floor and the **lower legs** to be perpendicular to floor (thighs may be slightly elevated above knees). If "no" refer to Chairs or Work Surfaces.		
9. **Feet** rest flat on the floor or are supported by a stable footrest. If "no" refer to Chairs, Work Surfaces.		

Notes:

SEATING–Consider these points when evaluating the chair	Y	N
10. **Backrest** provides support for your lower back (lumbar area).		
11. **Seat width** and **depth** accommodate the specific user (seat pan not too big/small).		
12. **Seat front** does not press against the back of your knees and lower legs (seat pan not too long).		
13. **Seat** has cushioning and is rounded with a "waterfall" front (no sharp edge).		
14. **Armrests,** if used, support both forearms while you perform computer tasks and they do not interfere with movement.		
"No" answers to any of these questions should prompt a review of Chairs.		

Notes:

KEYBOARD/INPUT DEVICE–Consider these points when evaluating the keyboard or pointing device. The keyboard/input device is designed or arranged for doing computer tasks so the	Y	N
15. **Keyboard/input device platform(s)** is stable and large enough to hold a keyboard and an input device.		
16. **Input device** (mouse or trackball) is located right next to your keyboard so it can be operated without reaching.		
17. **Input device** is easy to activate and the shape/size fits your hand (not too big/small).		
18. **Wrists** and **hands** do not rest on sharp or hard edges.		
"No" answers to any of these questions should prompt a review of Keyboards, Pointers, or Wrist Rests.		

Notes:

MONITOR–Consider these points when evaluating the monitor. The monitor is designed or arranged for computer tasks so the	Y	N
19. Top of the screen is at or below eye level so you can read it without bending your head or neck down/back.		
20. User with bifocals/trifocals can read the screen without bending the head or neck backward.		
21. Monitor distance allows you to read the screen without leaning your head, neck or trunk forward/backward.		
22. Monitor position is directly in front of you so you don't have to twist your head or neck.		
23. Glare (for example, from windows, lights) is not reflected on your screen which can cause you to assume an awkward posture to clearly see information on your screen.		
"No" answers to any of these questions should prompt a review of Monitors or Workstation Environment.		

Notes:

WORK AREA–Consider these points when evaluating the desk and workstation. The work area is designed or arranged for doing computer tasks so the	Y	N
24. Thighs have sufficient clearance space between the top of the thighs and your computer table/keyboard platform (thighs are not trapped).		
25. Legs and **feet** have sufficient clearance space under the work surface so you are able to get close enough to the keyboard/input device.		

Notes:

ACCESSORIES–Check to see if the	Y	N
26. Document holder, if provided, is stable and large enough to hold documents.		
27. Document holder, if provided, is placed at about the same height and distance as the monitor screen so there is little head movement, or need to re-focus, when you look from the document to the screen.		
28. Wrist/palm rest, if provided, is padded and free of sharp or square edges that push on your wrists.		
29. Wrist/palm rest, if provided, allows you to keep your forearms, wrists, and hands straight and in line when using the keyboard/input device.		
30. Telephone can be used with your head upright (not bent) and your shoulders relaxed (not elevated) if you do computer tasks at the same time.		
"No" answers to any of these questions should prompt a review of Work Surfaces, Document Holders, Wrist Rests or Telephones.		

Notes:

GENERAL	Y	N
31. Workstation and equipment have sufficient adjustability so you are in a safe working posture and can make occasional changes in posture while performing computer tasks.		
32. Computer workstation, components and accessories are maintained in serviceable condition and function properly.		
33. Computer tasks are organized in a way that allows you to vary tasks with other work activities, or to take micro-breaks or recovery pauses while at the computer workstation.		
"No" answers to any of these questions should prompt a review of Chairs, Work Surfaces, or Work Processes.		

Notes:

APPENDIX B

DETAILS AND ANALYSIS OF C-SECTION IN MAHMOOD ET AL. (2005)

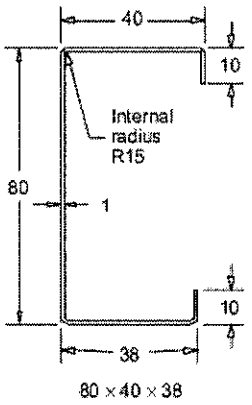

Figure B.1 Dimensions of C-section 80x40x38 based on Mahmood et al. (2005)

The section properties are as follows:

Web height, h	= 80mm
Top flange width, b1	= 40mm
Bottom flange width, b2	=38mm
Lip length, d	= 10mm
Lip angle (radians), θ	= 90° = 1.57 rad
Thickness, t	= 1mm
Area, A	= 271.6558mm^2
Young's modulus, E	= 200kN/mm^2
Poisson's ratio, ν	= 0.3
Yield stress, f_y	= 275N/mm^2
x-axis effective length, Kx	= 1
y-axis effective length, Ky	= 1
Torsion effective length, Kt	= 0.5 (assumption)
x-axis unbraced length, Lx	= 500mm
y-axis unbraced length, Ly	= 500mm
Torsion unbraced length, Lt	= 500mm
x-axis moment of inertia, I_x	= 533996.2428 mm^4
y-axis moment of inertia, I_y	= 5997.3822mm^4
Torsional constant, J	= 90.5519 mm^4

Title : Development of a column chart for C80x40x38 based on DSM in AISI (2004)

Consider the C80x40x38 with the elastic buckling analysis curve

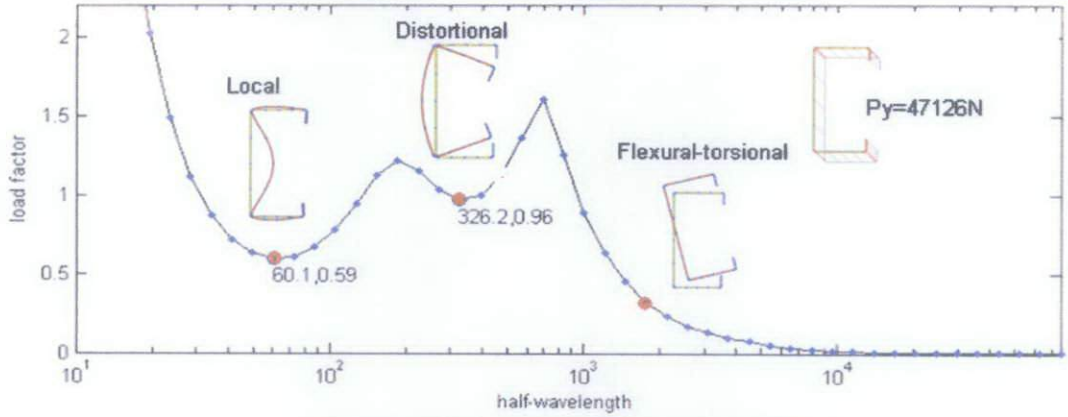

Figure B.2 Finite strip analysis for C80x40x38

Inputs from the finite strip analysis include:

P_y =	47126.81				
P_{crl} =	0.59369 Py	P_{crl} =	27978.72	L_{crl} =	60.1
P_{crd} =	0.9646 Py	P_{crd} =	45458.53	L_{crd}=	326.2

The finite strip analysis enforces a single half sine wave for the deformation along the length to develop the above figure. To develop a column chart one must determine how each of the buckling modes will behave without this restriction. Find P_{crl}, P_{crd}, P_{cre} as a function of length.

Local buckling (P_{crl}) as a function of length

For lengths longer than the local buckling minimum 60.1 local buckling will simply repeat itself up and down. Length shorter than 60.1 is not of interest, so it is assumed that the local buckling value is constant with length.

P_{crlp}=	27978.72	local buckling minimum from FSM
$P_{crl}(L)$=	P_{crlp}	local buckling does not change (even at short lengths)

Distortional buckling (P_{crd}) as a function of length

For lengths longer than the distortional buckling minimum 326.2 distortional buckling will [illegible] with multiple half-waves along the length.

[illegible] 45456.53 L_{crd}= 326.2 Distortional buckling minimum from FSM

$$P_{crd}(L) = P_{crpd} \quad \text{if } L \geq L_{crd}$$

$$P_{crd}(L) = P_{crpd} \cdot \left(\frac{L}{L_{crd}}\right)^{\ln\left(\frac{L}{L_{crd}}\right)} \quad \text{if } L < L_{crd}$$

Global buckling (P_{cre}) as a function of length

Global buckling is strongly dependent on length.

$$P_{cre}^2 \cong \propto \left(\frac{1}{L}\right)^2 + \beta \left(\frac{1}{L}\right)^4 \quad \text{if } L = L_x = L_t$$

Pick two points along the global buckling curve to fit to

L_{cr1}=	1215.9		L_{cr2}=	3112.1	
P_{cre1}=	0.62957 P_y=	29669.63	P_{cre2}=	0.1289 P_y=	6074.646

The 70th and 90th points are selected from FSM analysis. Any two points which are clearly in the global (lateral-torsional) buckling regime will do.

The constants $\propto$ and β are found via:

$$\propto = \frac{P_{cre1}^2 \cdot L_{cr1}^4 - P_{cre2}^2 \cdot L_{cr2}^4}{I_{cr1}^2 - I_{cr2}^2} = 1.9E+14$$

$$\beta = \frac{(P_{cre1}^2 \cdot L_{cr1}^2 - P_{cre2}^2 \cdot L_{cr2}^2) \cdot L_{cr1}^2 \cdot L_{cr2}^2}{L_{cr2}^2 - L_{cr1}^2} = 1.6E+21$$

$$P_{cre} = \sqrt{\propto \left(\frac{1}{L}\right)^2 + \beta \left(\frac{1}{L}\right)^4}$$

Buckling loads as a function of length are:

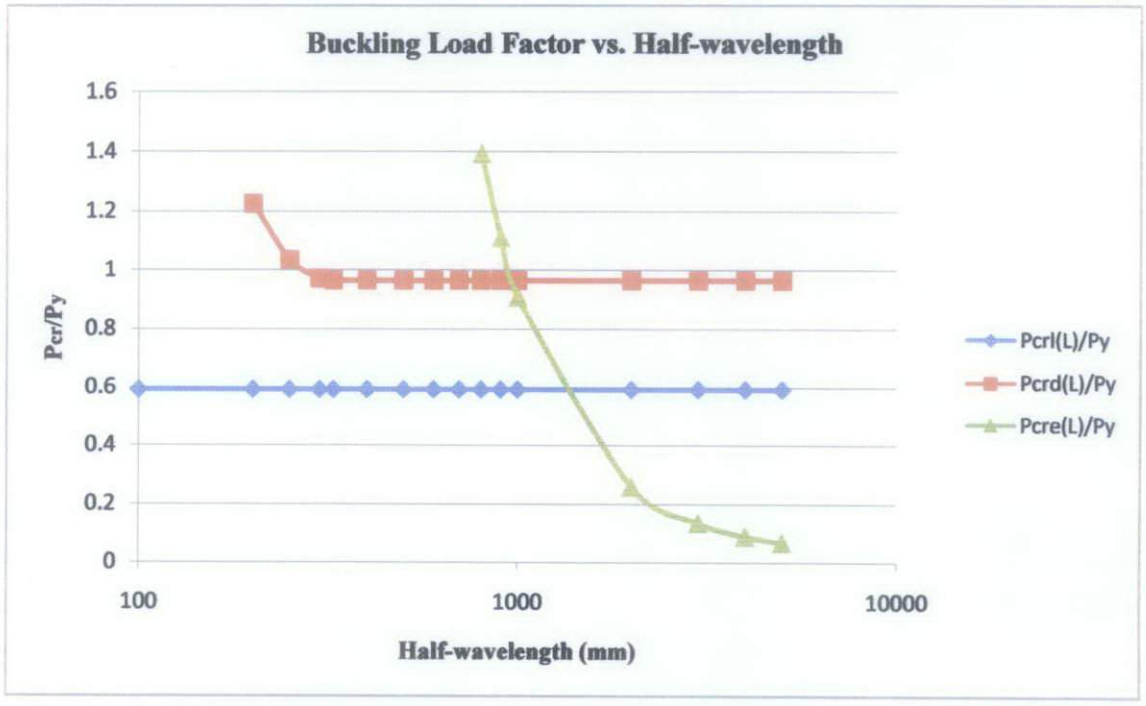

Figure B.3 Graph of buckling load factor vs. half-wavelength for C80x40x38

Developed column chart for C80x40x38

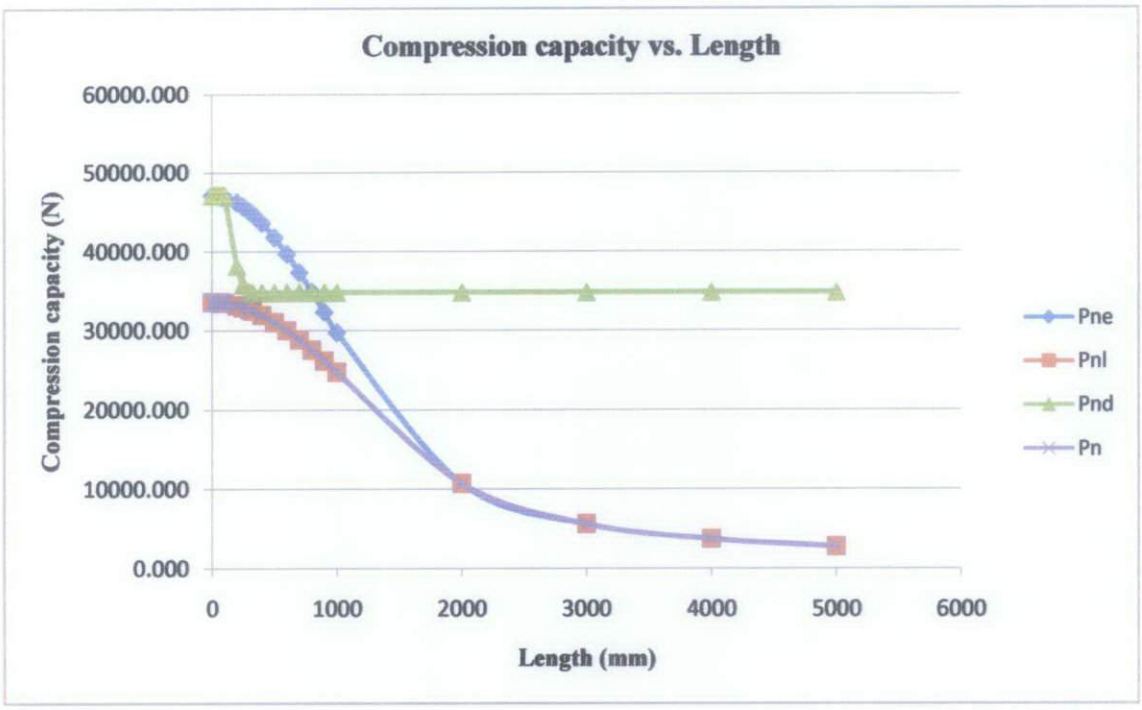

Figure B.4 Graph of compression capacity vs. member length for C80x40x38

Notes:

1) Local buckling dominates the actual column strength
2) The reduction due to local buckling is large even for short columns
3) Distortional buckling never controls in this section

APPENDIX C

DETAILS AND ANALYSIS OF INNOVATIVE STEEL COLUMN SECTIONS IN NARAYANAN ET AL. (2003)

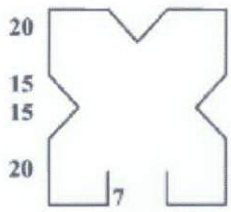

Column 1

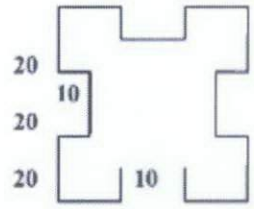

Column 2

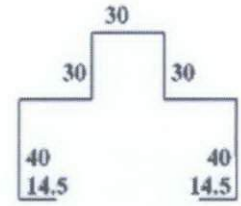

Column 6

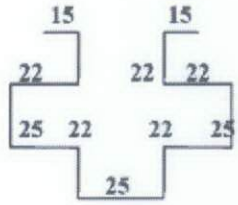

Column 7

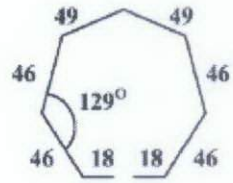

Column 15

Figure C.1 Section geometries of the innovative steel columns

Table C.1 Properties of steel column sections

Column number	Steel grade	Thickness (mm)	Gross area (mm^2)	Critical column slenderness ratio, L/r
1	550	0.80	211.2	43.0
2	550	0.80	240.0	45.5
6	550	0.95	247.0	44.4
7	550	0.95	267.0	45.8
15	250	1.14	362.5	28.6

itle: Development of a column chart for Column 1 based on DSM in AISI (2004)

onsider the Column 1 with the elastic buckling analysis curve

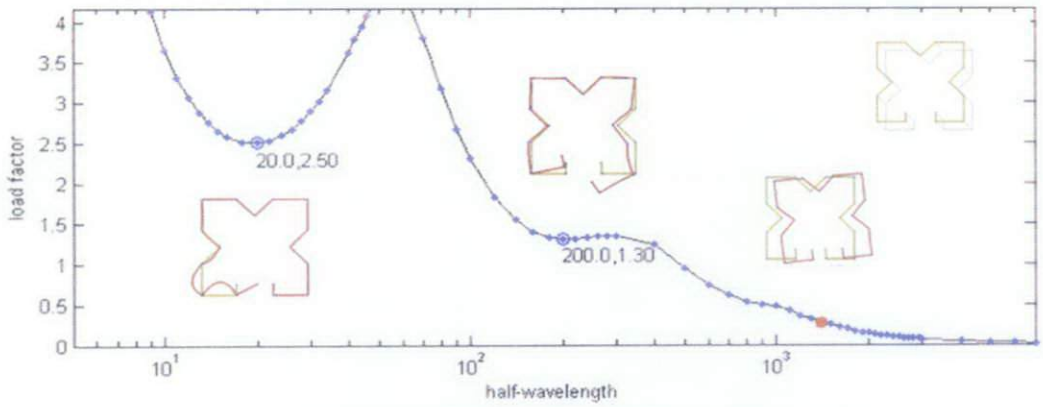

Figure C.2 Finite strip analysis for Column 1

nputs from the finite strip analysis include:

$_y$ =	117004.1				
crl =	2.5032 Py	Pcrl =	292885	Lcrl =	20
crd =	1.2988 Py	Pcrd =	151965	Lcrd=	200

he finite strip analysis enforces a single half sine wave for the deformation along the length to develop the above gure. To develop a column chart one must determine how each of the buckling modes will behave without this striction. Find Pcrl, Pcrd, Pcre as a function of length.

ocal buckling (Pcrl) as a function of length

or lengths longer than the local buckling minimum 20 local buckling will simply repeat itself up nd down. Length shorter than 20 is not of interest, so it is assumed that the local buckling value constant with length.

crlp=	292884.7	local buckling minimum from FSM
crl(L)=	Pcrlp	local buckling does not change (even at short lengths)

istortional buckling (Pcrd) as a function of length

or lengths longer than the distortional buckling minimum 200 distortional buckling will imply repeat with multiple half-waves along the length.

crdp=	151964.9	Lcrd=	200	Distortional buckling minimum from FSM

$$P_{crd}(L) = P_{crpd} \quad \text{if } L \geq L_{crd}$$

$$P_{crd}(L) = P_{crpd} \cdot \left(\frac{L}{L_{crd}}\right)^{\ln\left(\frac{L}{L_{crd}}\right)} \quad \text{if } L < L_{crd}$$

lobal buckling (P_{cre}) as a function of length

lobal buckling is strongly dependent on length.

$$_{re}^{2} \cong \propto \left(\frac{1}{L}\right)^{2} + \beta \left(\frac{1}{L}\right)^{4} \quad \text{if } L = L_{r} = L_{r}$$

ick two points along the global buckling curve to fit to

$_{cr1}$=	1400			L_{cr2}=	2000	
$_{cre1}$=	0.27427	P_y=	32090.72	P_{cre2}=	0.14 P_y=	16456.63

he 70th and 90th points are selected from FSM analysis. Any two points which are clearly in the global ateral-torsional) buckling regime will do.

he constants ∝ and β are found via:

$$_{} = \frac{P_{cre1}^{2} \cdot I_{cr1}^{4} - P_{cre2}^{2} \cdot I_{cr2}^{4}}{L_{cr1}^{2} - L_{cr2}^{2}} = 1.848E+14$$

$$_{} = \frac{(P_{cre1}^{2} \cdot L_{cr1}^{2} - P_{cre2}^{2} \cdot L_{cr2}^{2}) \cdot L_{cr1}^{2} \cdot L_{cr2}^{2}}{L_{cr2}^{2} - L_{cr1}^{2}} = 3.594E+21$$

$$_{cre} = \sqrt{\propto \left(\frac{1}{L_{}}\right)^{2} + \beta \left(\frac{1}{L_{}}\right)^{4}}$$

uckling loads as a function of length are:

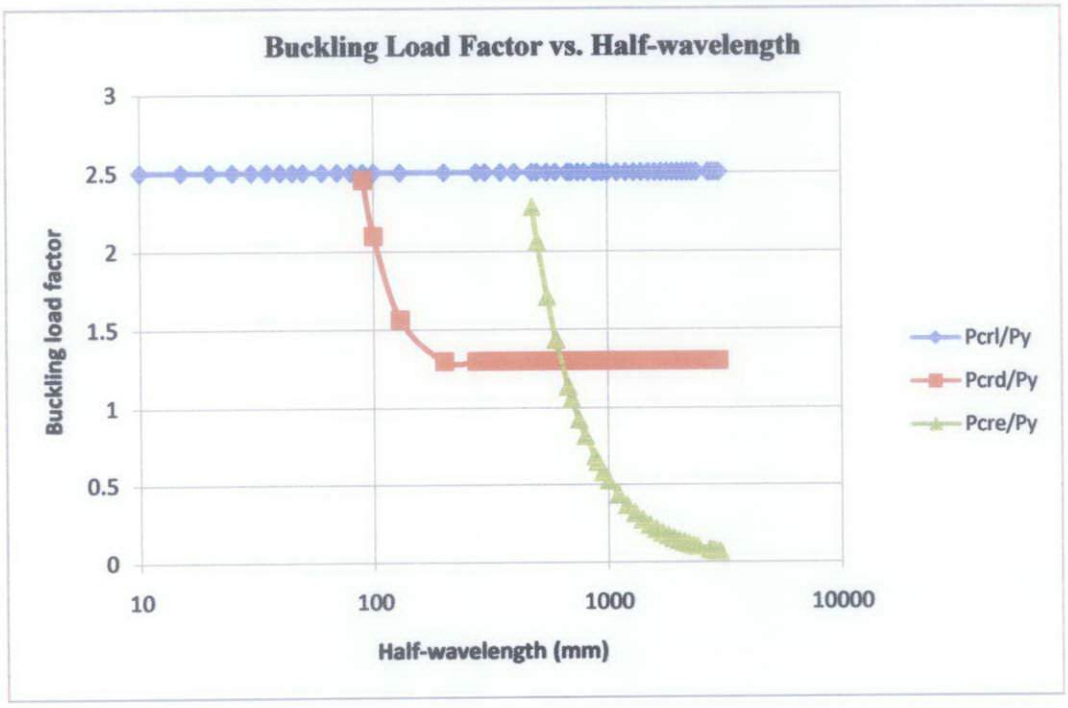

Figure C.3 Graph of buckling load factor vs. half-wavelength for Column 1

eveloped column chart for Column 1

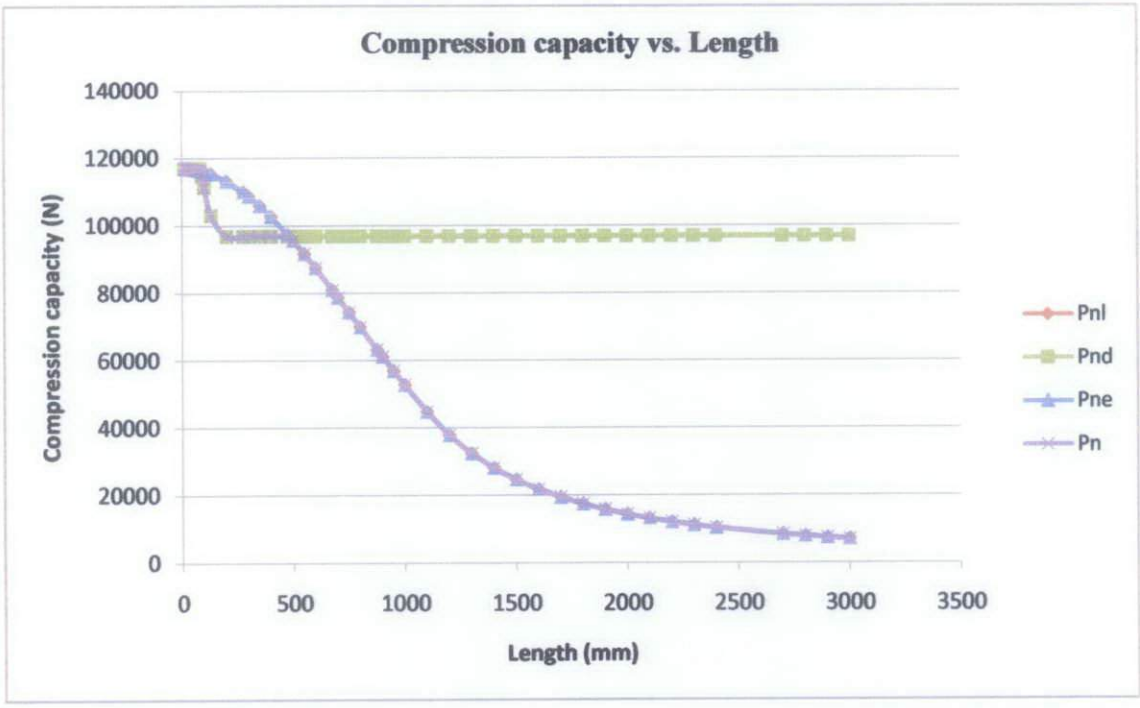

Figure C.4 Graph of compression capacity vs. member length for Column 1

lotes:

) Local and flexural buckling dominates column strength when column length is <70mm and >550mm

) Distortional buckling dominates column strength when column length is 70<L<550mm

APPENDIX D

DETAILS AND ANALYSIS OF LYSAGHT C-SECTIONS AND Z-SECTIONS

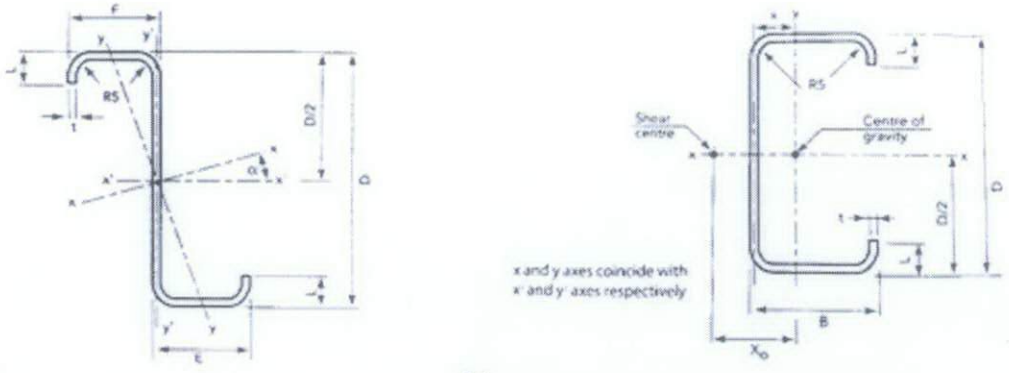

(a) (b)

Figure D.1 (a) Lysaght Z-section and (b) Lysaght C-section

Table D.1 Dimensions of Lysaght Z-section and C-section

Catalogue number	t (mm)	D (mm)	Mass per unit length (kg/m)	Zeds			Cees	
				E (mm)	F (mm)	L (mm)	B (mm)	L (mm)
Z/C 15015	1.5	152	3.56	65	61	16.5	64	15.5
Z/C 15019	1.9	152	4.49	65	61	17.5	64	16.5

Table D.2 Section properties of Lysaght Z-section

Product code	Full section properties												
	Principal axes						Axes perpendicular and parallel to web						
	Area	Second moment of area		Section modulus	Radius of gyration		Second moment of area		Product of moment of area	Section modulus		Radius of gyration	
	A	Ix	Iy	Zy	ry	α	Ix'	Iy'	Ix'y'	Zx'	Zy'	rx	ry
	mm^2	10^6mm^4	10^6mm^4	10^3mm^3	mm	°	10^6mm^4	10^6mm^4	10^6mm^4	10^3mm^3	10^3mm^3	mm	mm
Z15015	443	1.84	0.145	3.96	18.1	22.0	1.60	0.383	0.588	20.8	6.06	60.1	29.4
Z15019	561	2.32	0.184	5.02	18.1	22.1	2.01	0.487	0.744	26.1	7.73	59.9	29.5

Product code	Column properties		Effective section properties at yield stress	
	Torsion constant	Warping constant	Section modulus in bending	Area in compression
	J	Iw	Zx'e	Ae
	mm^4	10^6mm^6	10^3mm^3	mm^2
Z15015	332	1460	17.2	248
Z15019	675	1860	22.4	347

Table D.3 Section properties of Lysaght C-section

Full section properties									Column properties				Effective section properties at yield stress	
Product code	Area	Second moment of area		Section modulus		Radius of gyration		Centroid	Shear centre	Torsion constant	Warping constant	Monosym-metry section constant	Section modulus in bending	Area in compression
	A	Ix	Iy	Zx	Zy	rx	ry	x	x_o	J	Iw	Iw	Zx'e	Ae
	mm^2	10^6mm^4	10^6mm^4	10^3mm^3	10^3mm^3	mm	mm	mm	mm	mm^4	10^6mm^6	10^6mm^6	10^3mm^3	mm^2
C15015	443	1.61	0.237	21.1	5.29	60.2	23.1	18.4	46.9	332	1070	171	17.1	244
C15019	561	2.02	0.300	26.6	6.74	60.0	23.1	18.5	47.1	675	1370	170	21.8	340

Figure D.6 Failure mode for specimen Z15015 of 500 mm length

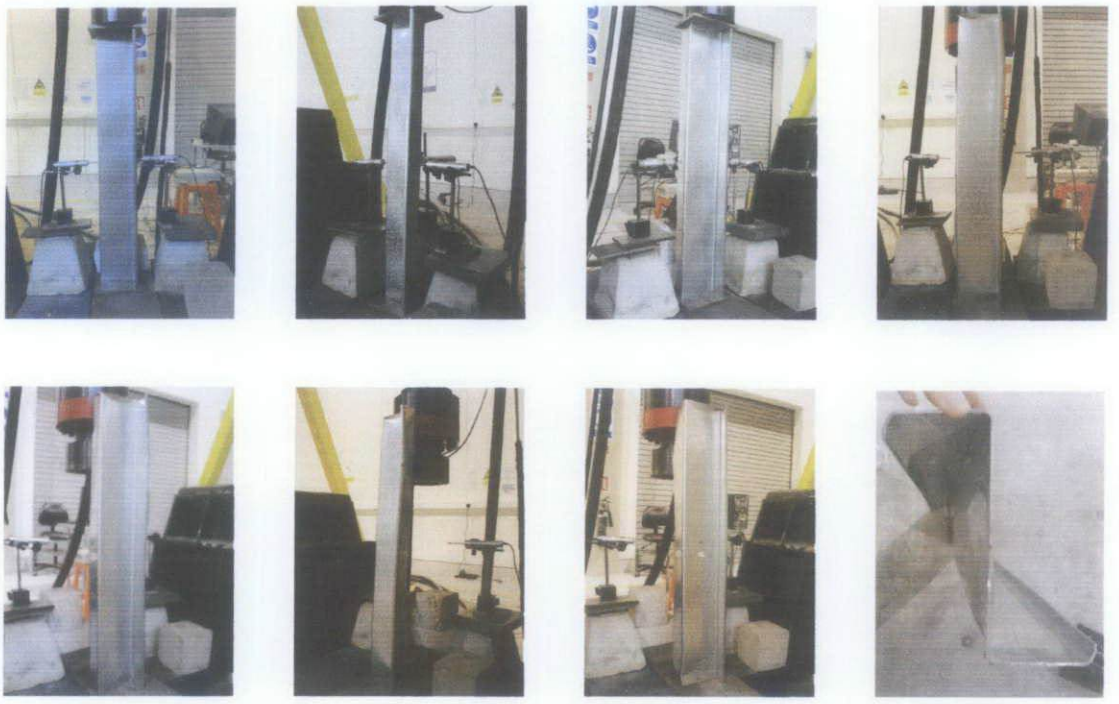

Figure D.7 Failure mode for specimen Z15015 of 1000 mm length

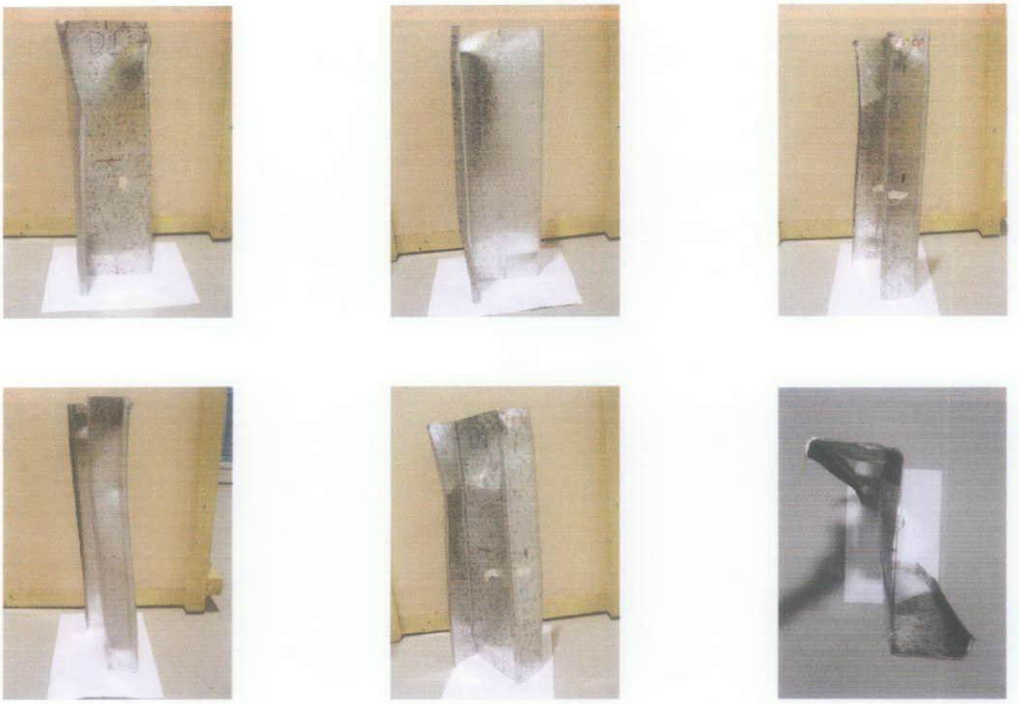

Figure D.8 Failure mode for specimen Z15019 of 500 mm length

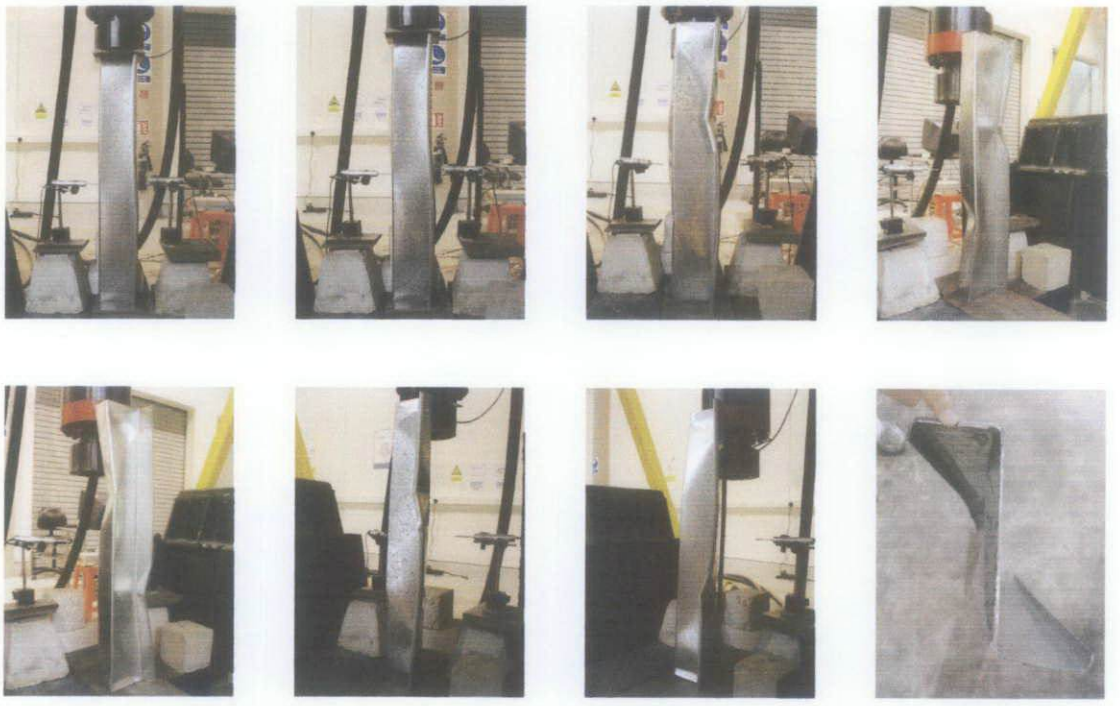

Figure D.9 Failure mode for specimen Z15019 of 1000 mm length

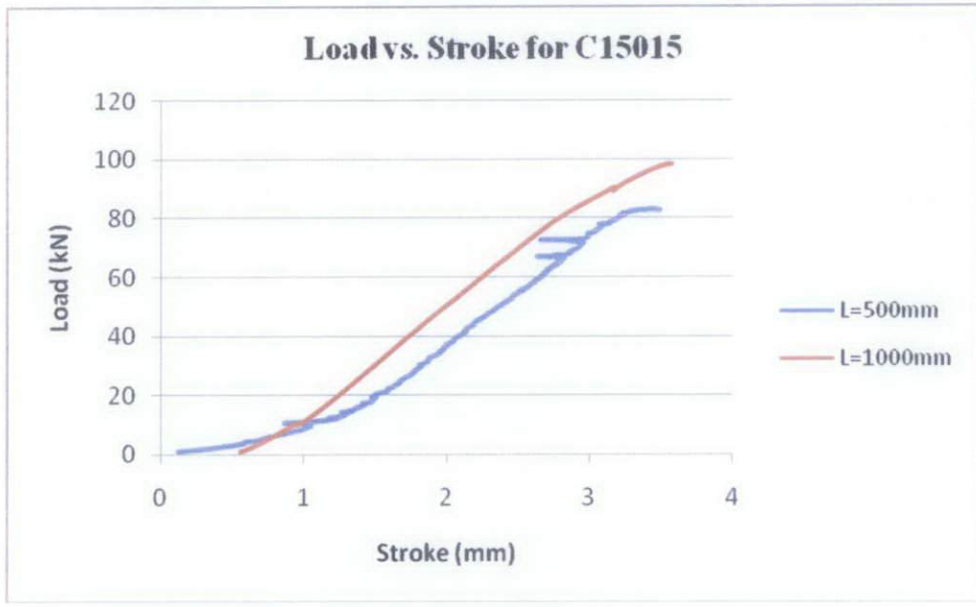

Figure D.10 Graph of load vs. stroke for specimen C15015 of 500mm and 1000mm length

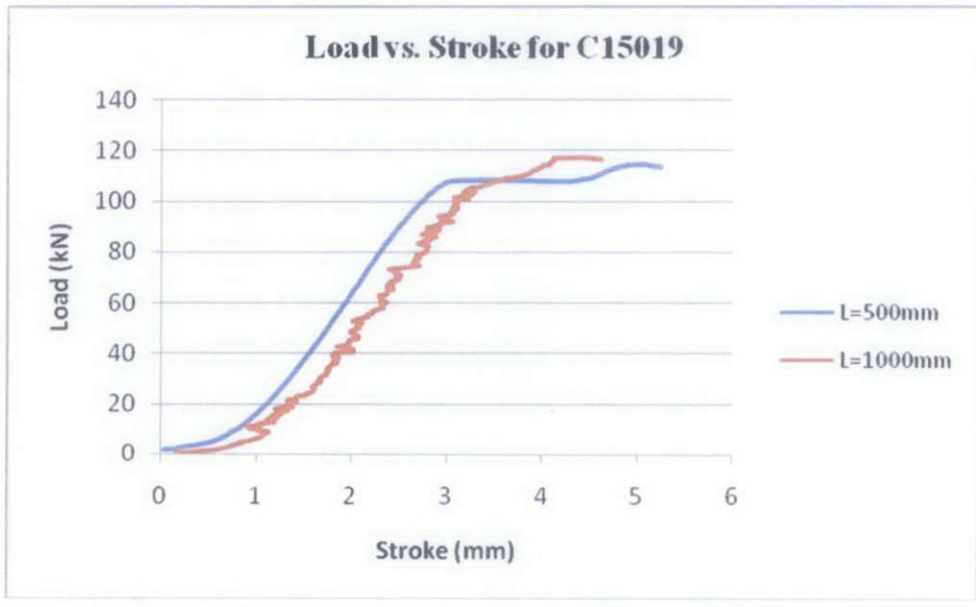

Figure D.11 Graph of load vs. stroke for specimen C15019 of 500mm and 1000mm length

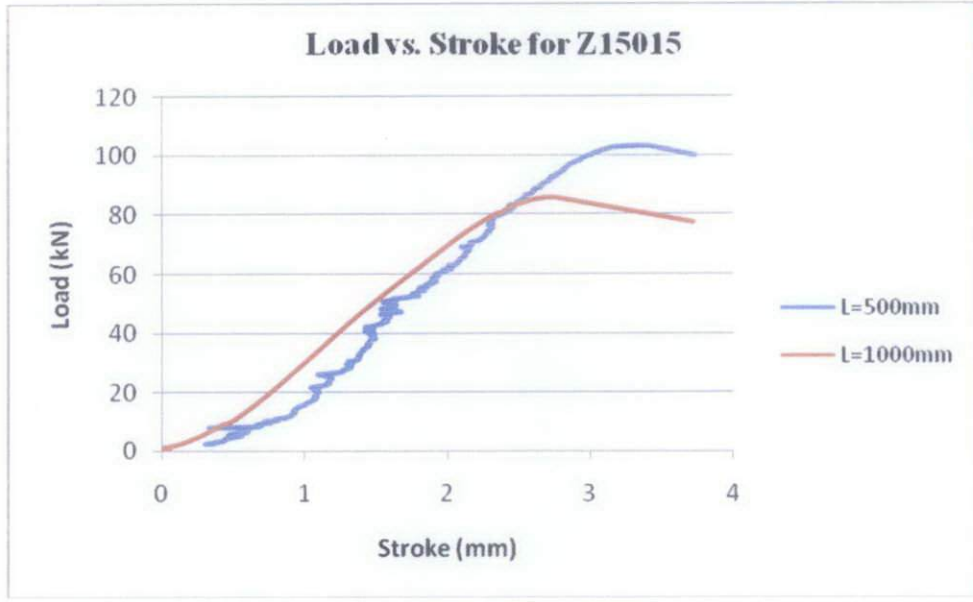

Figure D.12 Graph of load vs. stroke for specimen Z15015 of 500mm and 1000mm length

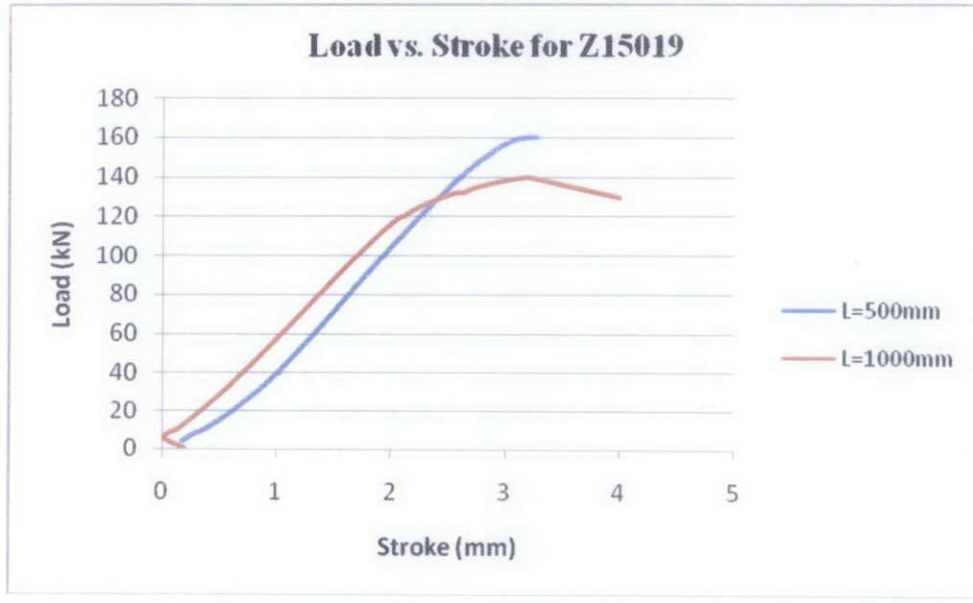

Figure D.13 Graph of load vs. stroke for specimen Z15019 of 500mm and 1000mm length

Title: Development of a column chart for C15015 based on DSM in AISI (2004)

Consider the C15015 with the elastic buckling analysis curve

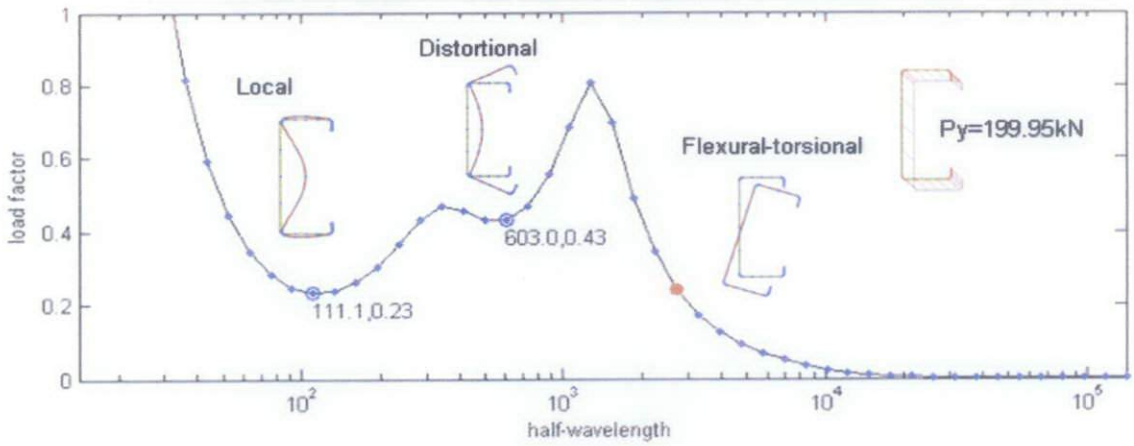

Figure D.14 Finite strip analysis for C15015

Inputs from the finite strip analysis include:

P_y =	199949.9				
P_{crl} =	0.23289 Py	P_{crl} =	46566.33	L_{crl} =	111.1
P_{crd} =	0.43024 Py	P_{crd} =	86026.45	L_{crd}=	603

The finite strip analysis enforces a single half sine wave for the deformation along the length to develop the above figure. To develop a column chart one must determine how each of the buckling modes will behave without this restriction. Find P_{crl}, P_{crd}, P_{cre} as a function of length.

Local buckling (P_{crl}) as a function of length

For lengths longer than the local buckling minimum 111.1 local buckling will simply repeat itself up and down. Length shorter than 111.1 is not of interest, so it is assumed that the local buckling value is constant with length.

P_{crlp}=	46566.33	local buckling minimum from FSM
$P_{crl}(L)$=	P_{crlp}	local buckling does not change (even at short lengths)

Distortional buckling (P_{crd}) as a function of length

For lengths longer than the distortional buckling minimum 603 distortional buckling will simply repeat with multiple half-waves along the length.

P_{crdp}= 86026.45 L_{crd}= 603 Distortional buckling minimum from FSM

$$P_{crd}(L) = P_{crpd} \quad \text{if } L \geq L_{crd}$$

86026.447

$$P_{crd}(L) = P_{crpd} \cdot \left(\frac{L}{L_{crd}}\right)^{\ln\left(\frac{1}{L_{crd}}\right)} \quad \text{if } L < L_{crd}$$

Global buckling (P_{cre}) as a function of length

Global buckling is strongly dependent on length.

$$P_{cre}^2 \cong \propto \left(\frac{1}{L}\right)^2 + \beta \left(\frac{1}{L}\right)^4 \quad \text{if } L = L_x = L_t$$

Pick two points along the global buckling curve to fit to

L_{cr1}=	3273.6			L_{cr2}=	8378.9		
P_{cre1}=	0.1735	P_y=	34691.31	P_{cre2}=	0.034419	P_y=	6882.076

The 70th and 90th points are selected from FSM analysis. Any two points which are clearly in the global (lateral-torsional) buckling regime will do.

The constants $\propto$ and β are found via:

$$\propto = \frac{P_{cre1}^2 \cdot L_{cr1}^4 - P_{cre2}^2 \cdot L_{cr2}^4}{L_{cr1}^2 - L_{cr2}^2} = 1.601E+15$$

$$\beta = \frac{(P_{cre1}^2 \cdot L_{cr1}^2 - P_{cre2}^2 \cdot L_{cr2}^2) \cdot L_{cr1}^2 \cdot L_{cr2}^2}{L_{cr2}^2 - L_{cr1}^2} = 1.211E+23$$

$$P_{cre} = \sqrt{\propto \left(\frac{1}{L}\right)^2 + \beta \left(\frac{1}{L}\right)^4}$$

Buckling loads as a function of length are:

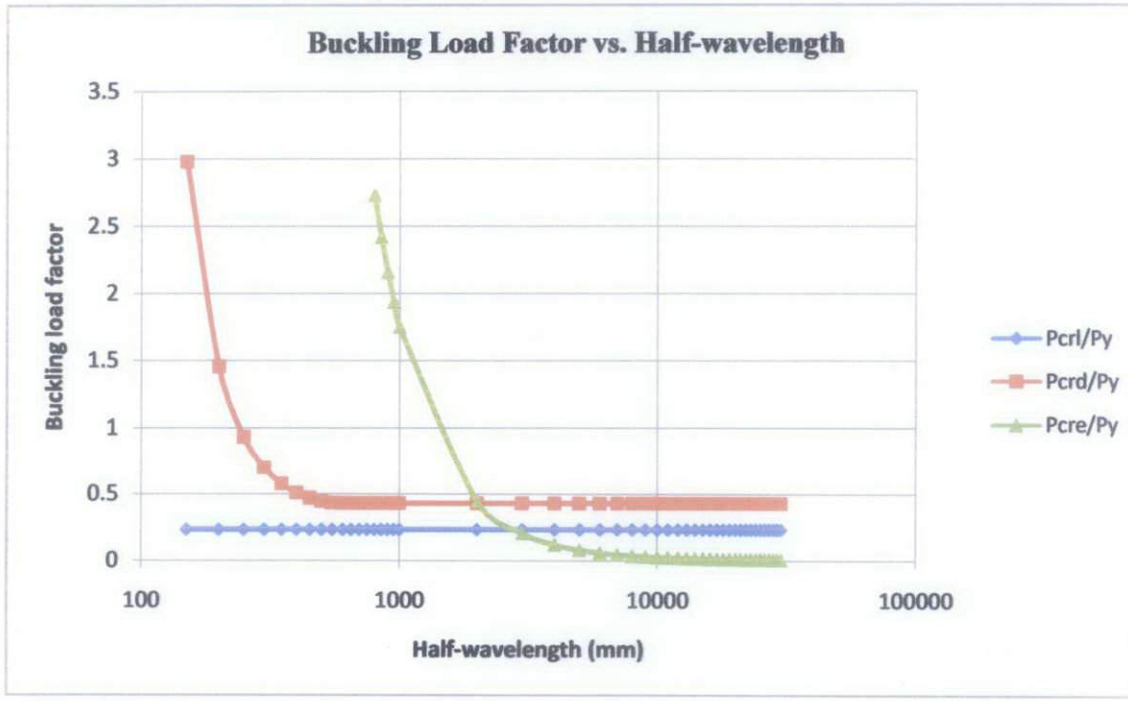

Figure D.15 Graph of buckling load factor vs. half-wavelength for C15015

Developed column chart for C15015

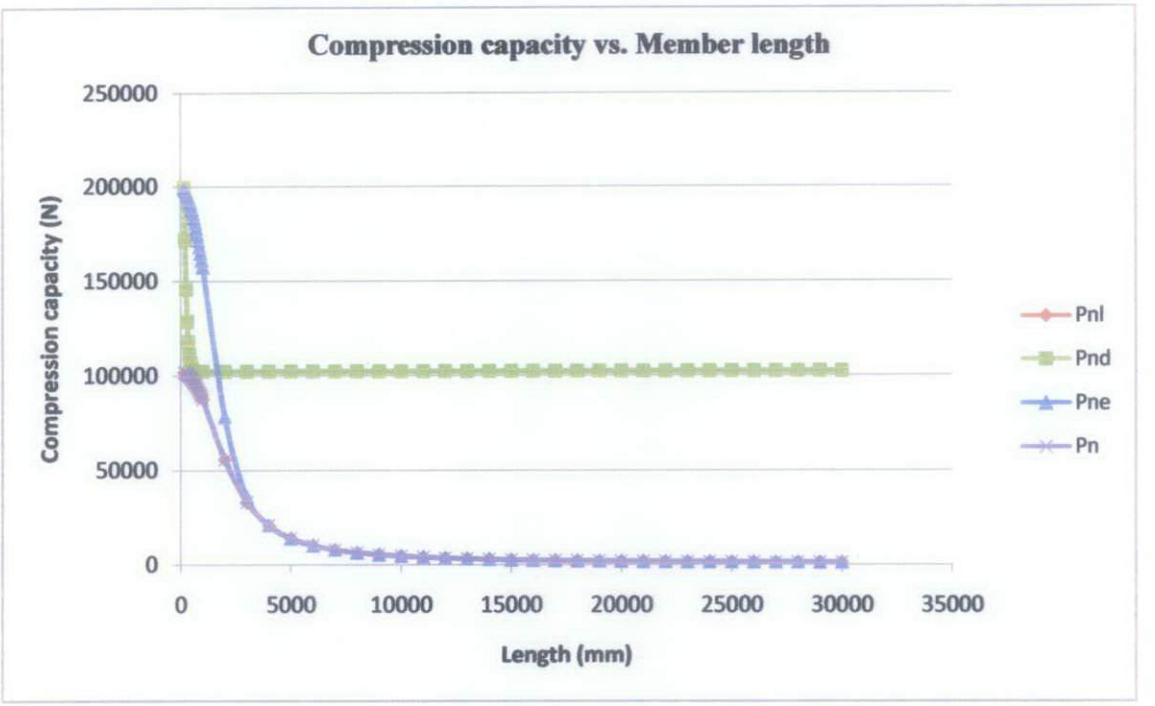

Figure D.16 Graph of compression capacity vs. member length for C15015

Notes:

1) Local buckling dominates the actual column strength

3) Distortional buckling never controls this section

2) The reduction due to local buckling is large even for short columns

Flexural buckling based on The European Code for the Design of Steel Structures (Eurocode 3) Part 1.3 (CEN, ENV 1993-1-3)

The effects of local buckling are taken into account by using effective section properties. The design buckling resistance for axial compression $N_{b,Rd}$ shall therefore be obtained from:

$$N_{b,Rd} = \frac{\chi A_{eff} f_{yb}}{\gamma_{M1}}$$

Where

A_{eff}= the effective area of the cross-section, obtained by assuming a uniform compressive stress $\sigma_{com,Ed}$ equal to f_{yb}/γ_{M1};

γ_{M1}= partial safety factor for buckling = 1.05;

χ = the appropriate value of the reduction factor for buckling resistance:

$$\chi = \frac{1}{\phi + \sqrt{\phi^2 + \bar{\lambda}^2}} \quad \chi \leq 1$$

where

$$\phi = 0.5\left[1 + \alpha\left(\bar{\lambda} - 0.2\right) + \bar{\lambda}^2\right]$$

α= imperfection factor

α= 0.34 for lipped C-section and lipped Z-section

$\bar{\lambda}$= the relative slenderness for flexural buckling about a given axis, determined as:

$$\bar{\lambda} = \frac{\lambda}{\lambda_1}\sqrt{\frac{A_{eff}}{A_g}}$$

where

$$\lambda = \frac{L}{i}$$

L= buckling length for flexural buckling about the relevant axis

i= the radius of gyration about the corresponding axis, based on the properties of the gross section.

$$\lambda_1 = \pi\sqrt{E/f_y}$$

Table D.2 Ultimate load based on Effective Width Method in Eurocode 3

Section	C15015	C15015	C15019	C15020	Z15015	Z15015	Z15019	Z15019
E	205000	205000	205000	205000	205000	205000	205000	205000
Py	450	450	450	450	528	528	514	514
I_{22}	238719	238719	303310.21	303310.21	146679.44	146679.44	186632.55	186632.55
A_g	444	444	563.582	563.582	444.3331	444.3331	563.582	563.582
A_{eff}	251.79435	251.79435	368.16633	368.16633	228.4399	228.4399	337.9019	337.9019
L_E	500	1000	500	1000	500	1000	500	1000
r	23.187398	23.187398	23.19877	23.19877	18.168969	18.168969	18.197643	18.197643
α	0.34	0.34	0.34	0.34	0.34	0.34	0.34	0.34
λ	21.563438	43.126875	21.552867	43.105734	27.519447	55.038895	27.476086	54.952172
λ_1	67.05336	67.05336	67.05336	67.05336	61.902736	61.902736	62.740105	62.740105
$\bar{\lambda}$	0.2421748	0.4843496	0.2597933	0.5195866	0.3187583	0.6375166	0.3390989	0.6781978
ϕ	0.536494	0.6656367	0.5439111	0.6893149	0.5709923	0.7775915	0.5811408	0.8112698
χ	0.8887981	0.671663	0.8720819	0.6441136	0.8163708	0.5608165	0.7974608	0.5351379
$N_{b,Rd}$	95911.863	72480.406	137601.93	101631.83	93778.666	64422.473	131908.81	88517.701

Effective Width Method in BS5950-5:1998

1. *K* factors for compression elements

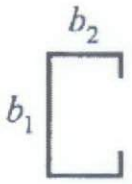

For lipped channel,

$$K_1 = 7 - \frac{1.8h}{0.15 + h} - 1.43h^3$$

$$K_2 = K_1 h^2 \left(\frac{t_1}{t_2}\right)^2$$

where
$h = b_2/b_1$
b_1, b_2 are the mid-line dimensions of the respective elements assuming rounded corners are replaced with the intersections of the flat elements;
t_1, t_2 are the thicknesses of element widths b_1 and b_2 respectively.

The *K* factors given refer to the element of width b_1 in all cases and are thus termed K_1. Where K_1 is less than 4 in the case of a stiffened element and 0.425 in the case of an unstiffened element, the value 4 or 0.425 may be used.

In the case of uniformly compressed members the corresponding *K* factor for elements of width b_2, which is thus termed K_2. Where K_2 is less than 4 or 0.425 as the case may be then the values 4 or 0.425 may be used.

2. Effective widths of plates with both edges supported (stiffened elements)

The ratio of effective width, b_{eff}, to full flat width, b, of an element under compression may be determined from the following:

for $f_c/p_{cr} \leq 0.123$ $\frac{b_{eff}}{b}=1$

for $f_c/p_{cr} > 0.123$ $\frac{b_{eff}}{b}=\left[1+14\left\{(f_c/p_{cr})^{1/2}-0.35\right\}^4\right]^{-0.2}$

Where

f_c is the compressive stress on the effective element;

p_{cr} is the local buckling stress of the element given by:

$$p_{cr} = 0.904EK\left(\frac{t}{b}\right)^2$$

where
K is the local buckling coefficient which depends on element type, section geometry;
t is the material thickness.

The effective width may be obtained from the product of the ratio b_{eff}/b and the actual element width.

3. Effective widths of plates with one edge supported (unstiffened elements)

The effective width, b_{eu}, of an unstiffened element under uniform compression may be obtained from the following:

$$b_{eu} = 0.89b_{eff} + 0.11b$$

where
b_{eff} is determined in accordance with **1** (the value of K may be taken as 0.425 for any unstiffened element);
b is the full flat width.

The effective width may be obtained from the product of the ratio b_{eu}/b and the actual element width.

4. Local buckling load

For the C-channel section, the effective width of each element, namely, web, flange and lip, can be calculated separately, and then the effective area A_{eff} of the section can be determined as:

$$A_{eff} = (b_{eff1} + 2b_{eff2} + 2b_{eff3})t$$

where

b_{eff1} is the effective web depth;

b_{eff2} is the effective flange length;

b_{eff3} is the effective lip length.

Finally, the local buckling load, P_{cs}, of the section is obtained as:

$$P_{cs} = p_y A_{eff}$$

where
p_y is the design strength.

5. Ultimate loads

For sections symmetrical about both principal axes or closed cross-sections which are not subject to torsional flexural buckling, or are braced against twisting, the buckling resistance under axial load, P_c, may be obtained from the following:

$$P_c = \frac{P_E P_{cs}}{\phi + \sqrt{\phi^2 - P_E P_{cs}}}$$

where

$$\phi = \frac{P_{cs} + (1+\eta)P_E}{2}$$

P_{cs} is the short strut capacity;

P_E is the minimum elastic flexural buckling load and is equal to:

$$P_E = \frac{\pi^2 EI}{L_E^2}$$

where
E is the modulus of elasticity;
I is the second moment of area of the cross-section about the critical axis;
L_E is the effective length of the member about the critical axis;

η is the Perry coefficient, such that:

for $L_E / r \leq 20$, $\eta = 0$

for $L_E / r > 20$, $\eta = 0.002(L_E/r - 20)$

where

r is the radius of gyration of the gross cross-section corresponding to P_E.

6. Ultimate load of Singly symmetrical sections

For sections symmetrical about a single axis and which are not subject to torsional flexural buckling, or which are braced against twisting, the effects of movement of the effective neutral axis should be taken into account in evaluation of the maximum load.

The buckling resistance, P'c, may then be evaluated from:

$$P'_c = \frac{M_c P_c}{(M_c + P_c e_s)}$$

where

M_c is the moment capacity having due regard to the direction of moment application;

Pc is the buckling resistance under axial load;
e_s is the distance between the geometric neutral axis of the gross cross-section and that of the effective cross-section.

The movement of the effective neutral axis may be calculated by determining the neutral axis position of the gross cross-section and that of the effective cross-section. In evaluation of the neutral axis position of the effective cross-section the effective portions should be positioned as shown in Figure D.20.

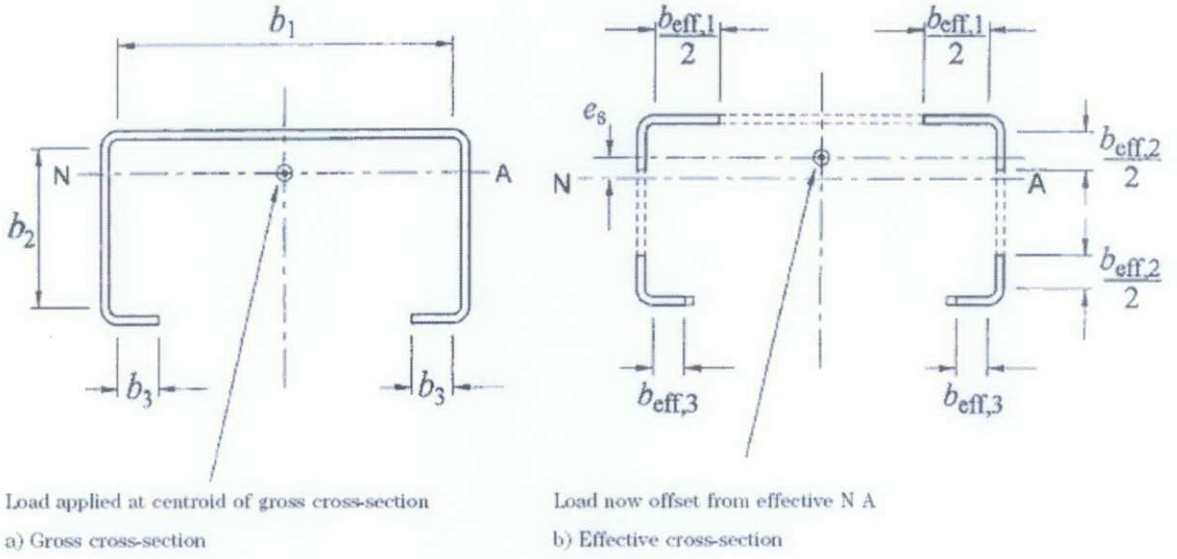

Figure D.20 Compression of singly symmetrical section (From BS5950-5:1998)

Title **Ultimate load based on Effective Width Method in BS5950-5:1998**

Section	Z15015	h	140.5	150.5
E	205000	b1	53.5	52
Py	528	b2	49.5	48
Izz	146679.44	d	10.75	15.75
LE	500	t	1.5	
r	18.168969	A	444.3331	

1. K factors for compression elements

K1	=	4.000
K2	=	4.000
K3	=	0.425

2. Effective widths of web

p_{cr}	=	84.491
f_c/p_{cr}	=	6.249
$\frac{b_{eff}}{b}$	=	0.320
b_{aff}	=	44.899

2. Effective widths of flange (b1)

p_{cr}	=	582.716
f_c/p_{cr}	=	0.906
$\frac{b_{eff}}{b}$	=	0.812
b_{aff}	=	43.428

2. Effective widths of flange (b2)

p_{cr}	=	680.698
f_c/p_{cr}	=	0.776
$\frac{b_{eff}}{b}$	=	0.861
b_{aff}	=	42.630

3. Effective widths of lip

p_{cr}	=	1533.475
f_c/p_{cr}	=	0.344
$\frac{b_{eff}}{b}$	=	0.991
b_{aff}	=	10.658
b_{eu}	=	10.668

4. Local buckling load

A_{eff}	=	228.440
P_{cs}	=	120616.2663

5. Ultimate load

P_E	=	1187087.835
η	=	0.015
Φ	=	662778.295
P_c	=	118634.044
CG	=	
CG'	=	
Mc	=	2151912.175
e_s	=	0.692
P'_c		114274.508